

# Reference Plasmid pHXB2\_D is an HIV-1 Molecular Clone that Exhibits Identical LTRs and a Single Integration Site Indicative of an HIV Provirus

Alejandro R. Gener (✉ [itspronouncedhenner@gmail.com](mailto:itspronouncedhenner@gmail.com))

Baylor College of Medicine <https://orcid.org/0000-0001-7875-2358>

**Wei Zou**

First Affiliated Hospital of Nanchang University

**Brian T. Foley**

Los Alamos National Laboratory

**Deborah P. Hyink**

Baylor College of Medicine

**Paul E. Klotman**

Baylor College of Medicine

---

## Research

**Keywords:** HIV-1, reagent verification, nanopore DNA sequencing, provirus, plasmid, sequence variability, resequencing, LTR phasing

**Posted Date:** April 6th, 2021

**DOI:** <https://doi.org/10.21203/rs.3.rs-382311/v1>

**License:**  This work is licensed under a Creative Commons Attribution 4.0 International License.

[Read Full License](#)

---

**Reference plasmid pHXB2\_D is an HIV-1 molecular clone that exhibits identical LTRs and a single integration site indicative of an HIV provirus**

Alejandro R. Gener<sup>1,2,3,4§</sup>, Wei Zou<sup>5</sup>, Brian T. Foley<sup>6</sup>, Deborah P. Hyink<sup>\*2</sup>, Paul E. Klotman<sup>\*1,2</sup>

<sup>1</sup>Integrative Molecular and Biomedical Sciences Program, Baylor College of Medicine, Houston, Texas, USA

<sup>2</sup>Margaret M. and Albert B. Alkek Department of Medicine, Nephrology, Baylor College of Medicine, Houston, Texas, USA

<sup>3</sup>Department of Genetics, MD Anderson Cancer Center, Houston, Texas, USA

<sup>4</sup>School of Medicine, Universidad Central del Caribe, Bayamón, Puerto Rico, USA

<sup>5</sup>Division of Infectious Diseases, the 1<sup>st</sup> Affiliated Hospital of Nanchang University, Nanchang, Jiangxi, China

<sup>6</sup>Theoretical Biology and Biophysics Group T-6, Los Alamos National Laboratory, Los Alamos, New Mexico, USA

\*Equal contributions.

§Corresponding author: Alejandro R. Gener

One Baylor Plaza

Mail Stop 710

Houston, Texas, 77030, USA

9045715562

[gener@bcm.edu](mailto:gener@bcm.edu) ; [itspronouncedhenner@gmail.com](mailto:itspronouncedhenner@gmail.com)

**Keywords:** HIV-1, reagent verification, nanopore DNA sequencing, provirus, plasmid, sequence variability, resequencing, LTR phasing

## 1 **Abstract**

2 **Objective:** To compare long-read nanopore DNA sequencing (DNA-seq) with short-read  
3 sequencing-by-synthesis for sequencing a full-length (e.g., non-deletion, nor reporter) HIV-1  
4 model provirus in plasmid pHXB2\_D.

5 **Design:** We sequenced pHXB2\_D and a control plasmid pNL4-3\_gag-pol( $\Delta$ 1443-4553)\_EGFP  
6 with long- and short-read DNA-seq, evaluating sample variability with resequencing (sequencing  
7 and mapping to reference HXB2) and *de novo* viral genome assembly.

8 **Methods:** We prepared pHXB2\_D and pNL4-3\_gag-pol( $\Delta$ 1443-4553)\_EGFP for long-read  
9 nanopore DNA-seq, varying DNA polymerases Taq (Sigma-Aldrich) and Long Amplicon (LA)  
10 Taq (Takara). Nanopore basecallers were compared. After aligning reads to the reference HXB2  
11 to evaluate sample coverage, we looked for variants. We next assembled reads into contigs,  
12 followed by finishing and polishing. We hired an external core to sequence-verify pHXB2\_D  
13 and pNL4-3\_gag-pol( $\Delta$ 1443-4553)\_EGFP with single-end 150 base-long Illumina reads, after  
14 masking sample identity.

15 **Results:** We achieved full-coverage (100%) of HXB2 HIV-1 from 5' to 3' long terminal repeats  
16 (LTRs), with median per-base coverage of over 9000x in one experiment on a single MinION  
17 flow cell. The longest HIV-spanning read to-date was generated, at a length of 11,487 bases,  
18 which included full-length HIV-1 and plasmid backbone with flanking host sequences  
19 supporting a single HXB2 integration event. We discovered 20 single nucleotide variants in  
20 pHXB2\_D compared to reference, verified by short-read DNA sequencing. There were no  
21 variants detected in the HIV-1 segments of pNL4-3\_gag-pol( $\Delta$ 1443-4553)\_EGFP.

22 **Conclusions:** Nanopore sequencing performed as-expected, phasing LTRs, and even covering  
23 full-length HIV. The discovery of variants in a reference plasmid demonstrates the need for

24 sequence verification moving forward, in line with calls from funding agencies for reagent  
25 verification. These results illustrate the utility of long-read DNA-seq to advance the study of  
26 HIV at single integration site resolution.

## 27 **Introduction**

28       Much of what we know about human acquired immunodeficiency syndrome (AIDS)  
29 came after isolating the causative agent – the human immunodeficiency virus type 1 (HIV-1) –  
30 and describing the viral genome information content. The HIV-1 isolate HXB2 (also known as  
31 HTLV-III and HIV-1<sub>LAI</sub> or LAV/BRU [1], [2]) was the first full-length replication-competent  
32 HIV genome sequenced [3]. Derivative clones commonly called “HXB2” are still used for *in*  
33 *vitro* infection assays, including RNA (almost always cDNA [4]) sequencing (**Figure 1A** and  
34 **Supplemental Table 1**). Despite the availability of the HXB2 HIV-1 reference sequence [3], no  
35 sequence is available for any complete and readily available HXB2 clone.

36       HIV clones were originally made by choosing non-cutter restriction enzymes to digest  
37 intact proviral sequences upstream and downstream of unknown integration sites from infected  
38 host cells while sparing HIV-1 sequence, followed by ligation into an *E. coli* cloning vector  
39 (plasmid) (**Figure 1B**), allowing for low-error (but not error-free) propagation [5]. These clones  
40 became available before tractable sequencing methods permitted routine sequence verification.  
41 As such, it was uncommon to sequence them. While funding agencies now require investigators  
42 to include in their proposals plans to validate their key reagents, these funders tend to leave the  
43 process up to investigators and may not always follow up on whether a given reagent is ever  
44 actually validated (or revalidated between changes of hand). Investigators do not regularly  
45 validate their clones, in part because there is no universally accepted standard. Instead, a



46 common practice is to assume a given clone, often kindly gifted from a colleague, is as reported.  
47 As such, we often do not truly know what we have been working with for 35+ years.

48 Making sense of the information from HIV sequencing experiments is complicated by  
49 many factors, including the cycling that all orterviruses [6] undergo between two major states (as  
50 infectious virion RNA and integrated proviral DNA **Figure 1B**), repetitive viral sequences like  
51 long terminal repeats (LTRs), non-integrated forms [7], rarity of integration events *in vivo*  
52 (reviewed in [8]), and alternative splicing of viral mRNAs [9]. Short-read DNA sequencing  
53 (<150 bases (bp) long in most reported experiments, but up to 500 bp for either Illumina (ILMN)  
54 sequencing-by-synthesis or <1,000 bp for chain termination sequencing) provides some  
55 information, but analyses require high coverage and/or extensive effort (non-exhaustive  
56 examples [10], [11]). These factors limit the ability to assign variants to specific loci within each  
57 provirus, as well as at the proviral integration site(s) (reviewed in [12]). Despite progress (HIV  
58 DNA) [13], (HIV RNA) [14], [15], [16], researchers have yet to observe the genome of HIV-1 as  
59 complete provirus (integrated DNA) in a single read, hindering locus-specific studies. To this  
60 end, current long-read DNA sequencing clearly surpasses the limitations of read length of  
61 leading next-generation/short-read sequencing platforms. Here we used the MinION sequencer  
62 to sequence HIV-1 plasmid pHXB2\_D in a pilot study focusing on coverage acquisition (as  
63 opposed to full-length sequencing), with the goal of evaluating the technology for future  
64 applications.

## 65 **Methods**

### 66 **HIV-1 plasmids**

67 A plasmid, “pHXB2\_D” (alternate names pHXB2, pHXB-2D), believed to contain the  
68 HIV-1 reference strain HXB2 [17] was acquired from the NIH AIDS Reagent and Reference  
69 Program (ARP) via BioServe. pHXB2\_D was believed to be a molecular clone (likely a  
70 restriction product of HXB2 proviral DNA inserted into an unknown cloning plasmid backbone)  
71 from one of the earliest clinical “HXB2” HIV-1 isolates. At the time of this work, it was  
72 unknown whether this plasmid was ever sequence-verified before or after the reference sequence  
73 for HXB2 was deposited.

74 The provenance of pNL4-3\_gag-pol( $\Delta$ 1443-4553)\_EGFP, a reporter construct of pNL4-3  
75 with a gag-pol deletion between base 1443 and 4553 is known. HIV-1 NL4-3 (pNL4-3) was a  
76 fusion of NY5 and LAV/HXB2 plasmids [18] that to our knowledge are not readily available.  
77 pEVd1443 [19] was a deletion construct made from pNL4-3 used to make several HIV-1  
78 transgenic animals, including the FVB/N-Tg(HIV)26AIn/PkltJ (The Jackson Laboratory stock  
79 No: 022354) “Tg26” mouse. The deletion in pEVd1443 was made by SphI cutting between  
80 d1443 and 1444 with binding site 1443-1448, and cutting at a Ball site at 4551-4556 with blunt  
81 cutting between 4553 and 4554. The EGFP cassette includes additional sequence upstream and  
82 downstream of EGFP coding sequence. SphI and Ball may still be used to excise EGFP cassette.  
83 A reporter construct was designed mimicking the pEVd1443 deletion: pNL4-3:  $\Delta$ G/P-EGFP  
84 [20]. Dr. Wei Zou rederived pNL4-3:  $\Delta$ G/P-EGFP at BCM [21]. Both constructs (plasmid and  
85 mouse) retained parts of gag and pol, with limited effects on protein-coding capacity, such as  
86 expression of p17 [22]. Based on Addgene naming conventions, we suggest pNL4-3\_gag-  
87 pol( $\Delta$ 1443-4553)\_EGFP to replace the previous name pNL4-3:  $\Delta$ G/P-EGFP for clarity.

## 88 **HIV-1 reference sequences**

89           The reference sequence of HXB2 is from the National Center for Biotechnology  
90 Information (NCBI), Genbank accession number K03455.1. It runs from the beginning of the 5'  
91 LTR to the end of the 3' LTR, and is 9,719 bp. This is similar to another HIV-1 reference that  
92 NCBI uses, AF033819.3. This is a 9,181 base HXB2-like sequence that starts at the 97 bp repeat  
93 in the 5'LTR, continues with the 5'UTR (U5), extends past the 3'UTR (U3) to the end of the 97  
94 bp repeat in 3'LTR, with one SNV at the *vpu* start codon aTg to aCg at position AF033819.3:560  
95 or K03455.1:6063. The reference sequence of NL4-3 is as a plasmid with accession number  
96 AF324493.1. It runs from the beginning of the 5' LTR to the end of the 3' LTR, spanning 9,709  
97 bp, and includes plasmid backbone with total length 14,825 bp.

## 98 **Long-read DNA sequencing**

99           A plasmid containing HXB2 was sequence-verified with long-read nanopore sequencing  
100 on a MinION Mk1B (Oxford Nanopore Technologies (ONT), Oxford, United Kingdom). Unless  
101 otherwise noted, reagents (and software) were purchased (or acquired) from ONT. Briefly, stock  
102 plasmid was diluted to 5 ng final amount in ultrapure water (as two samples) and processed with  
103 Rapid PCR Barcoding kit SQK-RPB004 along with 10 other barcoded samples (not discussed  
104 further in this manuscript) following ONT protocol RPB\_9059\_V1\_REVA\_08MAR2018  
105 (**Figure 1C**), a public description of which is here: [https://store.nanoporetech.com/us/sample-](https://store.nanoporetech.com/us/sample-prep/rapid-pcr-barcoding-kit.html)  
106 [prep/rapid-pcr-barcoding-kit.html](https://store.nanoporetech.com/us/sample-prep/rapid-pcr-barcoding-kit.html). Two DNA polymerases were evaluated (barcode 10 used  
107 high-fidelity LA (for “long amplicon”) Taq (Takara); barcode 11 Taq (Sigma-Aldrich). Libraries  
108 were loaded onto a MinION flow cell version R9.4.1 and a 48-hour sequencing run was  
109 completed with MinKNOW (version 1.10.11). Residual reads from subsequent runs were pooled

110 for final analyses. Long read data for pNL4-3\_gag-pol( $\Delta$ 1443-4553)\_EGFP was generated in  
111 other barcoded experiments (not shown).

112 Raw data was basecalled (converted from FAST5 to FASTQ format) with Albacore  
113 version 2.3.4 (older basecaller), Guppy version 2.3.1 (current official at time of work), and  
114 FlipFlop (Guppy development config). Mapping to reference was done with Minimap2 [23] and  
115 BWA-MEM [24], implemented in Galaxy (usegalaxy.org) [25]. Alignments (.bam and .bai files)  
116 were visualized in the Integrative Genomics Viewer [26] unless otherwise noted. For *de novo*  
117 assembly, demultiplexed basecalled reads were fed into Canu version 1.8 [27]. Genome size was  
118 estimated to be 16 Kb from agarose gel of undigested, but naturally degraded linearized  
119 pHXB2\_D (data not shown). SnapGene version 4.3.4 was used to manually annotate contigs  
120 from Canu. Blastn (NCBI) was used to identify unknown regions of pHXB2\_D. Polishing was  
121 performed on ONT-only assemblies with Medaka (<https://github.com/nanoporetech/medaka>), in  
122 Galaxy. Medaka models: r941\_min\_fast\_g303, r941\_min\_high\_g303, r941\_min\_high\_g330.  
123 Inference batch size (-b) = 100. The final pHXB2\_D assembly and other full-length HIV clones  
124 from the ARP were aligned to the most recent human reference genome (hg38) with Minimap2  
125 in Galaxy with the following parameters: Long assembly to reference mapping (-k19 -w19 -A1 -  
126 B19 -O39,81 -E3,1 -s200 -z200 --min-occ-floor=100).

## 127 **Statistics**

128 Two-tailed Mann-Whitney U tests were used to compare distributions in long-read data.  
129 P-values are reported over brackets delineating relevant comparisons. Calculations and graphing  
130 were done with GraphPad Prism for macOS version 8.0.2.

### 131 **Short-read DNA sequencing**

132 pHXB2\_D and control pNL4-3\_gag-pol( $\Delta$ 1443-4553)\_EGFP were provided as 35 ul at  
133 ~63 ng/ul to the Center for Computational & Integrative Biology DNA Core at Massachusetts  
134 General Hospital, an external DNA sequencing core specializing in high-throughput next  
135 generation (short-read) plasmid sequencing and assembly. Neither HXB2/pNL4-3 reference  
136 sequences nor pHXB2\_D/pNL4-3\_gag-pol( $\Delta$ 1443-4553)\_EGFP draft assemblies (from this  
137 work) were provided to core staff at the time of sequencing so that testing would remain masked.  
138 While the core's exact library prep is proprietary, multiplexed library prep and 150 single-end  
139 ILMN sequencing were most likely performed on a MiSeq with platform-specific reagents (V2  
140 chemistry, per their website) and barcoding. Data was returned as FASTQ. FASTQC [28] was  
141 used in Galaxy for in-house data quality control, and read lengths were all 142 bp per this tool.  
142 Mapping as above.

### 143 **Sequence comparisons**

144 We used MAFFT v7.475 [29], [30] to compare the LTR sequences of pHXB2\_D and  
145 HXB2, and pNL4-3 and pNL4-3\_gag-pol( $\Delta$ 1443-4553)\_EGFP. For cladistics, we used BLAST  
146 at HIV-DB ([https://www.hiv.lanl.gov/content/sequence/BASIC\\_BLAST/basic\\_blast.html](https://www.hiv.lanl.gov/content/sequence/BASIC_BLAST/basic_blast.html)) to  
147 find other HXB2-like genomes. The top 50 BLAST hits included many sequences pNL43 clones.  
148 pNL4-3 is an artificial recombinant of the NY5 clone with LAV and/or the HXB2 clone [18].  
149 The recombination point is marked by an EcoRI restriction site. We then made a multi-sequence  
150 alignment with the final pHXB2\_D assembly, the top BLAST hits, and the HIV-1 M group  
151 subtype reference set using GeneCutter  
152 ([https://www.hiv.lanl.gov/content/sequence/GENE\\_CUTTER/cutter.html](https://www.hiv.lanl.gov/content/sequence/GENE_CUTTER/cutter.html)), and built the  
153 maximum likelihood tree using IQ-tree

154 (<https://www.hiv.lanl.gov/content/sequence/IQTREE/iqtree.html>). pNL4-3\_gag-pol( $\Delta$ 1443-  
155 4553)\_EGFP was not included in the above trees because of absence of divergence from pNL4-3  
156 sequences outside of the EGFP cassette.

## 157 **Results**

158 Viewing mapped data in IGV, the long reads (median read length >2000 bp, **Figure 1E**)  
159 from both pHXB2\_D ONT experiments clearly covered each LTR (**Figure 1F, Supplemental**  
160 **Figures 1, 3**), while shorter reads collapsed into one of either LTR (**Figure 1F, Supplemental**  
161 **Figures 3D,3E**). This was also seen when long reads were shorter than LTRs (<600 bp).  
162 Mappers BWA-MEM and Minimap2 were chosen based on their ability to handle long and short  
163 reads. Other mappers were not evaluated. BWA-MEM mapped more ambiguously, piling  
164 partially mapped reads between each LTR; Minimap2 mapped with higher fidelity to reference  
165 without splitting reads. Coverage as sequencing depth was higher and more even from the  
166 higher-fidelity LA Taq library (**Supplemental Figure 1**). pNL4-3 was known to have distinct  
167 LTRs because it was a synthetic recombinant. The higher variant density in NL4-3 LTRs enabled  
168 mapping and phasing from short-read data only (**Supplemental Figure 2**).

169 We counted 20 single nucleotide variants (SNVs) in this reference clone of HXB2 (**Table**  
170 **1, Supplemental Table 3, Supplemental Figure 3E**). These mismatches were seen in all Canu  
171 assemblies (**Supplemental Figures 4A,4B**), verified in IGV and/or SnapGene, and were  
172 orthogonally verified by short-read sequencing performed by the external core given masked  
173 samples (**Supplemental Figure 3E**). These mismatches represent a ~0.21% divergence from  
174 reference HXB2 K03455.1 (20/9719), which was assumed to have perfect identity (0%  
175 divergence). Transitions were more common (14/20) (**Table 1**), coinciding with a previous

176 report of increased transitions over transversions in infection models, because transversions are  
177 more likely to be deleterious to viral replication (i.e.: to cause protein-coding changes) [31].  
178 Indeed, almost half (9/20) of the observed SNVs occurred in protein-coding regions, even though  
179 92% of HXB2 is coding (791/9719). Of those 9 SNVs in protein-coding regions, 4 caused non-  
180 synonymous mutations. One of those occurs in a region overlapping both gag and pol regions,  
181 however only pol exhibited a non-synonymous change from valine to isoleucine in p6, at  
182 position 2259 relative to HXB2. Other non-synonymous variants occurred at 4609 (in p31  
183 integrase, arginine to lysine), 7823 (in ASP antisense protein, glycine to arginine), and 9253 (in  
184 nef, isoleucine to valine). 11/20 SNVs were in LTRs (see **Supplemental Figure 3** for counting  
185 based on mapping); 8/20 of these would have been missed with mapping-only variant calling or  
186 consensus. The longest HIV-mapping read (**Figure 2**) phased 16/20 SNVs (failed at sites  
187 2,8,10,12, **Table 1**). pNL4-3\_gag-pol( $\Delta$ 1443-4553)\_EGFP did not have HIV-1 or plasmid  
188 backbone variants supported by long and short reads outside of the EGFP cassette.

189 We assembled the previously undefined plasmid pHXB2\_D (**Supplemental Figures**  
190 **4A,4B**). Canu's final output was a set of contiguous DNA sequences (contigs) as FASTA files. A  
191 consequence of assembling plasmid sequences with this tool was partial redundancy at contig  
192 ends (**Supplemental Figure 4C**). Manual end-trimming of contigs was performed in SnapGene  
193 based on an estimated length of 16 kb. Top blastn hits from barcode 10/LA Taq pHXB2  
194 basecalled with FlipFlop were as follows: for the main backbone (with origin of replication and  
195 antibiotic selection cassette for cloning), shuttle vector pTB101-CM DNA, complete sequence  
196 (based on pBR322), from 4352-8340; for the upstream element (relative to 5' LTR), Homo  
197 sapiens chromosome 3 clone RP11-83E7 map 3p, complete sequence from 58,052 to 59,165; for  
198 the downstream element, cloning vector pNHG-CapNM from 10,204 to 11,666. Other identified

199 elements included Enterobacteria phage SP6 (the SP6 promoter, per SnapGene’s “Detect  
200 common features”), complete sequence from 39,683 to 39,966. Identities of query to HXB2 and  
201 hits were all approximately 99%. The MGH CCIB DNA Core’s proprietary *de novo* UltraCycler  
202 v1.0 assembler (Brian Seed and Huajun Wang, unpublished) was able to assemble both 5’ and 3’  
203 LTRs with short-read data only but may have collapsed SNVs into an artificial single consensus.  
204 Long-read mapping and assembly (and polished assemblies) orthogonally validated LTRs and  
205 supported a single HIV-1 HXB2\_D haplotype (**Supplemental Figure 4,6**). A final LTR-phased  
206 and annotated assembly leveraging short and long reads is provided as pHXB2\_D  
207 Genbank:MW079479 (embargoed until publication). Importantly, for pHXB2\_D, each LTR was  
208 identical, which is distinct from the current HXB2 (K03455.1) (**Figure 3A**). Compared to pNL4-  
209 3\_gag-pol( $\Delta$ 1443-4553)\_EGFP (ACCESSION\_TBD), each LTR was distinct, but identical to  
210 pNL4-3’s distinct 5’ and 3’ LTRs (AF324493.1) (**Figures 3B,6**).

211 To determine whether pHXB2\_D was an isolated provirus (as opposed to a cDNA clone),  
212 the pHXB2\_D assembly was aligned to the current human reference hg38, returning a single  
213 complete insertion site on 3p24.3 (**Figure 4A, Supplemental Table 2**). As expected, our pNL4-  
214 3\_gag-pol( $\Delta$ 1443-4553)\_EGFP had homology arms from two chromosomes (**Figures 4B,6,**  
215 **Supplemental Table 2**). We sought to put our pHXB2\_D assembly into context of other HXB2-  
216 like references available (**Figure 5**). pHXB2\_D (red) clusters closely with HXB2 reference  
217 (K03455) and related clone sequences (green). pNL4-3 clones in blue. The LTR-masked HIV-  
218 spanning segment of pHXB2\_D is most homologous to B.FR.1983.DM461230 and  
219 B.FR.1983.CS793683, which are identical except for areas in *nef* and a GFP insertion (verified  
220 by *blastn*). This finding suggests they were from the same stock. HIV-1 M group subtype  
221 reference set (HIV Sequence Database) was added to put HXB2s and pNL4-3 clones into



222 perspective. HXB2 (believed to be a complete isolate) and NL4-3 (synthetic clone based on two  
223 early isolates [18]) are examples of HIV type 1 (HIV-1), group M, subgroup B.

224 As previously reported [32], per-read variability in ONT data was higher near  
225 homopolymers (runs of the same base) (**Supplemental Figure 5A**). For the datasets generated in  
226 the present study, homopolymers were counted and classified as continuous (unbroken run of a  
227 given nucleobase) vs. discontinuous (broken run of a given nucleobase) (**Supplemental Figures**  
228 **5B,5D,5F,5H**). A/T (2 hydrogen bonds; 2H) and G/C (3 hydrogen bonds; 3H) were evaluated.  
229 Because runs longer than 4 or 5 were rare in these datasets, it was impossible to evaluate longer  
230 homopolymers. A simple calculation  $Abs(\Delta) = Abs(\#homopolymers_{Reference} -$   
231  $\#homopolymers_{assembly})$  helped to evaluate the performance of basecallers, such that better  
232 basecallers had smaller  $Abs(\Delta)$  (**Supplemental Figures 5C,5E,5G,5I,5K**). At the level of  
233 consensus (made from sequences mapped to reference HXB2), homopolymers contributed few,  
234 if any, obvious errors. A special case of homopolymer, dimer runs, was noted to cause persistent  
235 errors regardless of ONT basecaller (**Supplemental Figures 5J,5K**). While dips occurred at  
236 certain points near homopolymers, the consensus did not change much at the sequencing depth  
237 used in this study for either barcoded pHXB2\_D samples (**Supplemental Figures 1,3,4**).  
238 Another interpretation is that homopolymers tend to seem truncated with ONT, with more reads  
239 in support of shorter homopolymers. Canu assemblies showed basecaller-dependent variability  
240 (**Supplemental Table 3**). That said, newer basecallers tended to produce fewer and smaller per-  
241 read truncations. Assemblies without polishing did not correct all homopolymer truncations  
242 (**Supplemental Figure 4A**). Polishing assemblies tended to correct these toward the final  
243 pHXB2\_D assembly (**Supplemental Figures 4B,6**). Data from polished ONT-only assemblies  
244 and short-read sequencing do not support the truncations (gaps relative to reference) suggested

245 by unpolished ONT-only assemblies, representing a known current limitation of ONT. These are  
246 not the same as the 20 SNVs supported by BOTH long- and short-read sequencing performed in  
247 this study. The ratio of per-read deletions to per-read insertions (DEL/INS) was much higher for  
248 SNVs occurring at homopolymers and near the same base, and this difference was maintained  
249 between all basecallers used (**Supplemental Figure 5L**). These changes created more  
250 problematic (longer) homopolymers.

## 251 **Discussion**

252 This work represents the first instance of complete and unambiguous sequencing of HIV-  
253 1 provirus as plasmid and contributed to the identification of single nucleotide variants which  
254 may not have been easily determined using other sequencing modalities, illustrating the  
255 importance of validating molecular reagents in their entirety, and with complementary  
256 approaches. Nanopore sequencing surpassed the read length limitations of traditional sequencing  
257 modalities used for HIV such as Sanger sequencing and sequencing-by-synthesis by at least two  
258 orders of magnitude. Other long-read DNA sequencing technologies such as PacBio's zero-mode  
259 waveguide DNA sequencing were not evaluated in this work, but in principle would be  
260 interchangeable for nanopore sequencing. Paired-end sequencing (as either DNA-seq or RNA-  
261 seq) was not evaluated in this work, but has shown promise phasing LTRs in our hands [33]–  
262 [35].

## 263 **First complete pass over all HIV information in reference plasmid pHXB2\_D**

264 HIV provirus is believed to occur naturally as one or a few copies of reverse-transcribed  
265 DNA forms integrated into the host nuclear genome. Depending on where integration occurs,  
266 local GC or AT content might cause problems for detecting integrants with PCR. HIV also has

267 conserved transitions from areas of higher GC content (~60%) to content approximating average  
268 human GC content (~40%). To limit PCR sequencing bias and to accommodate for the potential  
269 heterogeneity of HIV sequences, we fractionated whole sample directly (as opposed to PCR-  
270 barcoding select amplicons) with tagmentation provided in the Rapid PCR-Barcoding kit (ONT).  
271 Tagmentation in this workd used transposon-mediated cleavage and ligation of barcode adapters  
272 for later PCR amplification. A consequence of this fractionation was a distribution of reads  
273 (**Figure 1E**) shorter than longer reads reported elsewhere for ONT experiments [36]. Based on  
274 this distribution and the level of coverage, it was expected that HIV might be covered from end  
275 to end, but this would have been exceptional. That said, an example is presented here (**Figure 2**).  
276 The provirus status of pHXB2\_D is supported by recovery of both upstream and downstream  
277 homology arms which map to a single human integration site.

### 278 **Long reads enable LTR phasing and HIV haplotype definition**

279 We created 6 assemblies for pHXB2\_D from ONT-only data (**Supplemental Figure 4**),  
280 each with a common set of 20 SNVs (11 in LTRs), and final assemblies (a single HIV-1  
281 HXB2\_D haplotype; a single HIV-1 NL4-3\_gag-pol( $\Delta$ 1443-4553)\_EGFP haplotype) leveraging  
282 long- and short-read data. The external core's *de novo* assembly pipeline identified the same 20  
283 SNVs, and variants in the LTRs were supported by ONT unambiguously. That the core's  
284 assembler was able to phase LTR variants in these samples may have been because the samples  
285 had high amounts of the same upstream and downstream sequences because of coming from one  
286 plasmid. The core's assembler thus may have had additional sequencing information at the edges  
287 of HXB2, helping it to map deeper into each LTR. This approach would likely fail in samples  
288 with multiple integrations (as in various animal models of HIV disease [37]), which have  
289 unknown upstream and downstream sequences, or in samples from natural human infection,

290 which is well known to exhibit multiple pseudo-random integration sites between cells [38],  
291 [39], but with mostly single integration events per cell [8]. Inverse PCR (iPCR) is an alternative  
292 method [40] with its own issues (e.g., PCR biases, HIV concatemers, host repeats). While current  
293 PCR reagents have extended the range of what can be seen with iPCR, current approaches are  
294 likewise limited by long DNA extraction methods, sample amount, and remain to be optimized.  
295 If coverage is sufficient ( $\geq 10$  reads in non-homopolymers and non-dimer runs), long-read  
296 sequencing can provide linked variant information to individual integration sites. Identical 5' and  
297 '3 LTRs (**Figure 3**) in the context of a single integration event (**Figure 4A**) support this integrant  
298 being a *bona fide* provirus [41]. Other proviruses also had identical LTR pairs (**Supplemental**  
299 **Table 2**). Technical limitations such as PCR errors before earlier sequencing may explain the  
300 variability in the HXB2 reference LTRs. These were sequenced at a time before paired-end 150  
301 or long-read DNA-seq were available to phase LTRs, raising the possibility that these LTRs  
302 were incorrectly annotated by depositors assuming identity and copy-and-pasting the sequence of  
303 one LTR for both without being able to unambiguously resolve each LTR.

#### 304 **Mutations in a reference HIV-1 plasmid illustrate the need for reagent verification**

305 Up until 2020, HIV had been the most studied human pathogen, but HIV reagents are not  
306 routinely re(verified). The pHXB2\_D sequenced was allegedly a reference plasmid, with  
307 unknown divergence between the published reference HXB2. Three independent experiments  
308 (two long-read with PCR-barcoded libraries made with regular and long-amplicon Taq master  
309 mixes, one short-read) yielded at least 20 single nucleotide variants in pHXB2\_D which differed  
310 from the HXB2 reference sequence (**Table 1, Supplemental Figure 3**), which were also  
311 concordant across the three basecallers used (**Supplemental Table 3**) and are therefore not PCR  
312 errors. By leveraging long reads with the MinION, we were able to find mutations in highly

313 repetitive LTRs relative to HXB2 Genbank:K03455.1 which are often assumed (but until now  
314 never proven) to be identical (**Table 1, Figure 1, Supplemental Figures 1, 3E**), as well as  
315 mutations in protein-coding regions (**Table 1**). We were also able to confirm that the backbone  
316 of this plasmid is from pSP62 [17], a pBR322 derivative with the SP6 promoter [42], aiding in  
317 the continued use of this important reagent, and illustrating the need of full-length reagent  
318 validation moving forward. We suggest that all clinical reagents (e.g., vectors) be sequence-  
319 verified at the level of single-molecule sequencing as standard quality control to protect against  
320 sample heterogeneity.

### 321 **Improvement in ONT basecallers over time**

322       Albacore, Guppy, and FlipFlop basecallers were compared. Each produced reads of  
323 similar length distributions (relative to polymerase used), while Guppy and FlipFlop produced  
324 improved and best performance relative to quality score distributions (**Figure 1D**). Interestingly,  
325 while read length distributions were affected by fidelity of polymerases evaluated in this work,  
326 mean quality distributions were not. This is important because of the differences in cost between  
327 higher fidelity Taq and classic Taq enzymes. That said, higher fidelity LA Taq produced much  
328 higher coverage compared to Taq (**Supplemental Figure 1**). In consideration of library prep,  
329 choice of enzyme used should be based on the desired read-length distribution and coverage.  
330 Regarding read mapping, the increase in mean quality score between these basecallers improved  
331 overall mapping, in part by facilitating demultiplexing, resulting in approximately ~10%  
332 increases number of reads in barcoded libraries before mapping (shift in reads from unclassified  
333 to a given barcode). FlipFlop tended to handle homopolymers better than previous basecallers  
334 (**Supplemental Figures 5,6**). Homopolymers in HXB2 tended to exhibit apparent deletions near  
335 5' ends of homopolymers (upstream due to technical artifact from mapping), but because

336 consensus is conserved (example, at least 80% of base in called read set is identical to reference),  
337 and because short-read data lacks INDELS at these sites, it is unlikely that any of these  
338 homopolymer deletions are real in these experiments. Dimer runs – stretches of repeating 2-mers  
339 (pronounced “two-mers”) – proved challenging regardless of basecaller. Mapping as above may  
340 be used to aid in manually calling these when they occur. Albacore is currently deprecated, and  
341 current versions of Guppy now incorporate a version of FlipFlop called Guppy High-ACcuracy  
342 (HAC). Guppy HAC and subsequence versions were not evaluated in this work. Polishing is  
343 becoming standard practice for processing assemblies from ONT data because it redresses most  
344 homopolymer errors propagated into long-read-only assemblies. The best manually finished and  
345 polished contig had 1 error out of 16,722 bases, illustrating the utility of ONT hardware when  
346 paired with burgeoning software.

## 347 **Conclusions**

348 HIV informatics, the study of HIV sequence information, has been limited by the  
349 common assumption that sequence fidelity exists between reference genomes available in  
350 sequence databases and similarly named HIV clones. Modern DNA sequencing methods, such as  
351 long- and short-read sequencing, are available to redress this issue. Long-read sequencing fills in  
352 gaps left behind by short-read interrogation of HIV-1. Current limitations of the approaches used  
353 in the present work to study HIV are 1.) the cost of long-read sequencing, regardless of platform,  
354 compared to the cheaper short reads from sequencing-by-synthesis, 2.) long DNA extraction  
355 methods in diseased tissue (Gener, unpublished), and 3.) the lower per-base accuracy (low-mid  
356 90’s with ONT vs. 98-99% with ILMN or newer PacBio HiFi), including difficulty near  
357 homopolymers and dimer runs (**Supplemental Figure 5**). A nontrivial but redressable limitation

358 is availability of personnel trained to prepare sequencing libraries, to run sequencing, and to  
359 analyze results. As the price of long-read sequencing decreases, hardware and software used in  
360 basecalling and library protocols improve, and with the advent of more user-friendly tools, the  
361 cost of obtaining usable data from long reads will become negligible compared to the ability to  
362 answer historically intractable questions. This work raises the possibility of being able to detect  
363 at least some recombination events, in a reference-free manner requiring only the comparison of  
364 LTRs from the same integrants (**Figure 6**). We suggest that pHXB2\_D and pNL4-3 constructs  
365 may be used as negative and positive controls for the development of such screens. While other  
366 HIV reference proviral clones were reported to have identical LTR pairs, this remains to be  
367 tested in other clones, since other clones were generated with shorter sequencing methods. For  
368 example, pNL4-3\_gag-pol( $\Delta$ 1443-4553)\_EGFP had distinct LTRs as a plasmid. However, if an  
369 NL4-3 virus is made from pNL4-3, the LTR sequences would homogenize to pNL4-3's 3' LTR  
370 sequence. Future work will include optimizing DNA extraction protocols with the goal of  
371 capturing higher-coverage fuller glimpses of each HIV proviral integration site in *in vivo* HIV  
372 models and patient samples. This work has broad implications for all cells infected by both  
373 integrating and non-integrating viruses, and for the characterization of targeted regions in the  
374 genome which may be recalcitrant to previous sequencing methods. Long-read sequencing is an  
375 important emerging tool defining the post-scaffold genomic era, allowing for the characterization  
376 of anatomical landmarks of hosts and pathogens at the genomic scale.

## 377 **Declarations**

### 378 **List of Abbreviations**

379 HIV-1, human immunodeficiency virus.

380 PCR, polymerase chain reaction.

381 ONT, Oxford Nanopore Technologies; nanopore sequencing.

382 RNA-seq, usually refers to cDNA sequencing, unless otherwise specified (e.g., native

383 RNA-seq is not cDNA sequencing).

384 cDNA, reverse-transcribed “copy” DNA from single-stranded RNA templates. cDNA is

385 usually double-stranded DNA.

386 DNA-seq, DNA sequencing.

387 EGFP, enhanced green fluorescent protein.

388 LTR, long terminal repeat.

389 R, R repeat (a 97bp region in the LTR).

390 STEM, science, technology, engineering, math.

391 DNA, deoxyribonucleic acid.

392 RNA, ribonucleic acid.

393 LA, Long Amplicon.

394 SNV, single nucleotide variant.

395 AIDS, human acquired immunodeficiency syndrome.

396 mRNA, messenger RNA. These are usually 5' capped and polyadenylated in human

397 tissues.

398 BCM, Baylor College of Medicine.

399 IGV, Integrative Genomics Viewer.



400 bp, bases long.  
401 Kb, kilobases long.  
402 ASP, antisense protein.  
403 MGH CCIB, Center for Computational & Integrative Biology DNA Core at  
404 Massachusetts General Hospital.  
405 2H, two hydrogen bonds, as in A-T, A-U.  
406 3H, three hydrogen bonds, as in G-C.  
407 iPCR, inverse PCR.  
408 INDELS, insertions and/or deletions.  
409 ILMN, Illumina short-read DNA sequencing-by-synthesis.  
410 HiFi, High-fidelity.  
411 Abs(), absolute value.  
412 RRE, rev-response element.  
413 LANL, Los Alamos National Laboratory.

#### 414 **Ethics Approval**

415 This work did not include human or animal subjects. Nanopore libraries for this  
416 work were prepared in their entirety by ARG in a Biosafety Level 2 laboratory on main campus  
417 at Baylor College of Medicine (BCM). Nanopore sequencing was completed between April and  
418 May of 2018 as two of several control experiments included in the Student Genomics pilot run  
419 (**Supplemental Information**). Short-read sequencing was completed in April 2019.

#### 420 **Consent to publish**

421 All authors give their consent to publish the current work, pending peer review and  
422 acceptance.

423 **Availability of data and materials.**

424           The sequence for pHXB2\_D will be made available after publication with Genbank  
425 accession number MW079479 (embargoed until publication). We suggest this as a replacement  
426 for K03455.1 since MW079479 will have phased LTRs. pNL4-3\_gag-pol( $\Delta$ 1443-4553)\_EGFP  
427 will be deposited in Genbank as well. Both plasmids will be made available to the community  
428 through the AIDS Reagent Program. Sequencing data will be deposited into GEO. **Available**  
429 **additional files:** Albacore basecalled barcode 10, Guppy basecalled barcode 10, FlipFlop  
430 basecalled barcode 10, Albacore basecalled barcode 11, Guppy basecalled barcode 11, FlipFlop  
431 basecalled barcode 11, Minimap2 and BWA-MEM alignments (.bam and .bai), Clipboards from  
432 points of interest (verified SNVs; n=20), .dna files of contigs (n=6), MGH data (raw + contig),  
433 Supplemental Tables, Supplemental Figures.

434 **Competing interests**

435           ARG received travel bursaries from Oxford Nanopore Technologies (ONT). The present  
436 work was completed independently of ONT. Other authors declare no conflicts of interest.

437 **Funding**

438           This work was funded in part by institutional support from Baylor College of Medicine;  
439 the Human Genome Sequencing Center at Baylor College of Medicine; private funding by Bob  
440 Ostendorf, CEO of East Coast Oils, Inc., Jacksonville, Florida; ARG's own private funding,  
441 including Student Genomics (manuscripts in prep). Compute resources from the Computational  
442 and Integrative Biomedical Research Center at BCM ("sphere" cluster managed by Dr. Steven  
443 Ludtke) and the Department of Molecular and Human Genetics at BCM ("taco" cluster managed  
444 by Mr. Tanner Beck and Dr. Charles Lin) greatly facilitated the completion of this work. ARG  
445 has also received the PFLAG of Jacksonville scholarship for multiple years.

446 **Authors' contributions**

447 ARG conceived of this project, performed experiments, analyzed results, and drafted the  
448 manuscript. WZ rederived pNL4-3\_gag-pol( $\Delta$ 1443-4553)\_EGFP. All authors discussed data and  
449 edited the manuscript. ARG and PK provided funding.

450 **Acknowledgements**

451 As part of a summer bioinformatics internship in the Paul E. Klotman Laboratory at  
452 Baylor College of Medicine, Akash Naik supervised by ARG performed *in silico* mapping  
453 analyses/experiments, generated and/or aided in the synthesis of **Supplemental Figure 4**, and  
454 assisted in writing relevant portions, discussing, and editing this manuscript. During a second  
455 summer internship with American Physician Scientists Association Virtual Summer Research  
456 Program, the following students were supervised by ARG helped to create **Figure 1A** and  
457 **Supplemental Table 1**: Yini Liang, Kirk Niekamp, Maliha Jeba, Delmarie M. Rivera  
458 Rodríguez. Orthogonal sequence verification was performed as a service by staff at the Center  
459 for Computational & Integrative Biology DNA Core at Massachusetts General Hospital, Boston,  
460 MA, USA.

461 We would like to thank the staff at the DNA Core for their exceptional services,  
462 including expert analyses and rapid turnaround time. We would like to thank Drs. Steven  
463 Richards, Qingchang Meng and the staff of the Human Genome Sequencing Center Research  
464 (HGSC) and Development (R&D) team for their earlier support in nanopore adoption. We would  
465 like to thank the team at Oxford Nanopore Technologies for their timely improvements and  
466 continued R&D. I would also like to thank Ms. Taneasha Monique Washington (current) and  
467 former members of the Paul E. Klotman lab, Dr. Gokul C. Das and Alexander Batista. I would

468 like to thank Dr. Alana Canupp and the late Dr. Jim Maruniak for their early interest in my  
469 scientific development, and for the passion that they show in everything that they do.

470 **References**

- 471 [1] F. Barré-Sinoussi *et al.*, “Isolation of a T-lymphotropic retrovirus from a patient at risk for  
472 acquired immune deficiency syndrome (AIDS).,” *Science*, vol. 220, no. 4599, pp. 868–  
473 871, May 1983, doi: 10.1126/science.6189183.
- 474 [2] S. Wain-Hobson *et al.*, “LAV revisited: origins of the early HIV-1 isolates from Institut  
475 Pasteur.,” *Science*, vol. 252, no. 5008, pp. 961–965, May 1991, doi:  
476 10.1126/science.2035026.
- 477 [3] L. Ratner *et al.*, “Complete nucleotide sequence of the AIDS virus, HTLV-III.,” *Nature*,  
478 vol. 313, no. 6000, pp. 277–284, Jan. 1985, doi: 10.1038/313277a0.
- 479 [4] A. R. Gener and J. T. Kimata, “Full-coverage native RNA sequencing of HIV-1 viruses,”  
480 *bioRxiv*, p. 845610, Jan. 2019, doi: 10.1101/845610.
- 481 [5] G. M. Shaw, B. H. Hahn, S. K. Arya, J. E. Groopman, R. C. Gallo, and F. Wong-Staal,  
482 “Molecular characterization of human T-cell leukemia (lymphotropic) virus type III in the  
483 acquired immune deficiency syndrome.,” *Science*, vol. 226, no. 4679, pp. 1165–1171,  
484 Dec. 1984, doi: 10.1126/science.6095449.
- 485 [6] M. Krupovic *et al.*, “Ortervirales: New Virus Order Unifying Five Families of Reverse-  
486 Transcribing Viruses,” *J. Virol.*, vol. 92, no. 12, pp. e00515-18, May 2018, doi:  
487 10.1128/JVI.00515-18.
- 488 [7] E. H. Graf *et al.*, “Elite suppressors harbor low levels of integrated HIV DNA and high  
489 levels of 2-LTR circular HIV DNA compared to HIV+ patients on and off HAART,”  
490 *PLoS Pathog.*, vol. 7, no. 2, 2011, doi: 10.1371/journal.ppat.1001300.
- 491 [8] Y. Ito *et al.*, “Number of infection events per cell during HIV-1 cell-free infection,” *Sci.*  
492 *Rep.*, vol. 7, no. 1, p. 6559, 2017, doi: 10.1038/s41598-017-03954-9.

- 493 [9] I. Cuesta, A. Mari, A. Ocampo, C. Miralles, S. Pérez-castro, and M. M. Thomson,  
494 “Sequence Analysis of In Vivo -Expressed HIV-1 Spliced RNAs Reveals the Usage of  
495 New and Unusual Splice Sites by Viruses of Different Subtypes,” pp. 1–24, 2016, doi:  
496 10.1371/journal.pone.0158525.
- 497 [10] C. Wymant *et al.*, “Easy and accurate reconstruction of whole HIV genomes from short-  
498 read sequence data with shiver,” *Virus Evol.*, vol. 4, no. 1, pp. 1–13, 2018, doi:  
499 10.1093/ve/vey007.
- 500 [11] K. M. Bruner *et al.*, “A quantitative approach for measuring the reservoir of latent HIV-1  
501 proviruses,” *Nature*, vol. 566, no. 7742, pp. 120–125, 2019, doi: 10.1038/s41586-019-  
502 0898-8.
- 503 [12] M. R. Pinzone and U. O’Doherty, “Measuring integrated HIV DNA ex vivo and in vitro  
504 provides insights about how reservoirs are formed and maintained,” *Retrovirology*, vol.  
505 15, no. 1, pp. 1–12, 2018, doi: 10.1186/s12977-018-0396-3.
- 506 [13] K. B. Einkauf *et al.*, “Intact HIV-1 proviruses accumulate at distinct chromosomal  
507 positions during prolonged antiretroviral therapy Find the latest version : Intact HIV-1  
508 proviruses accumulate at distinct chromosomal positions during prolonged antiretroviral  
509 therapy,” vol. 129, no. 3, pp. 988–998, 2019.
- 510 [14] D. Bonsall *et al.*, “THAA0101 - HIV genotyping and phylogenetics in the HPTN 071  
511 (PopART) study: Validation of a high-throughput sequencing assay for viral load  
512 quantification, genotyping, resistance testing and high-resolution transmission  
513 networking,” in *22nd International AIDS Conference (AIDS2018)*, 2018, p. Oral Abstract.
- 514 [15] A. N. Banin *et al.*, “Development of a Versatile, Near Full Genome Amplification and  
515 Sequencing Approach for a Broad Variety of HIV-1 Group M Variants,” *Viruses*, vol. 11,

- 516 no. 4, p. 317, Apr. 2019, doi: 10.3390/v11040317.
- 517 [16] N. Nguyen Quang *et al.*, “Dynamic nanopore long-read sequencing analysis of HIV-1  
518 splicing events during the early steps of infection,” *Retrovirology*, vol. 17, no. 1, p. 25,  
519 2020, doi: 10.1186/s12977-020-00533-1.
- 520 [17] A. G. Fisher, E. Collalti, L. Ratner, R. C. Gallo, and F. Wong-Staal, “A molecular clone of  
521 HTLV-III with biological activity,” *Nature*, vol. 316, no. 6025, pp. 262–265, 1985, doi:  
522 10.1038/316262a0.
- 523 [18] A. Adachi *et al.*, “Production of acquired immunodeficiency syndrome-associated  
524 retrovirus in human and nonhuman cells transfected with an infectious molecular clone.,”  
525 *J. Virol.*, vol. 59, no. 2, pp. 284–91, 1986.
- 526 [19] P. Dickie *et al.*, “HIV-associated nephropathy in transgenic mice expressing HIV-1  
527 genes,” *Virology*, 1991. [Online]. Available: [http://ac.els-cdn.com/0042682291907595/1-](http://ac.els-cdn.com/0042682291907595/1-s2.0-0042682291907595-main.pdf?_tid=8f811f10-d10c-11e5-82e8-00000aacb35e&acdnat=1455228938_33d4226549c6410971ced1c4c3573a44)  
528 [s2.0-0042682291907595-main.pdf?\\_tid=8f811f10-d10c-11e5-82e8-](http://ac.els-cdn.com/0042682291907595/1-s2.0-0042682291907595-main.pdf?_tid=8f811f10-d10c-11e5-82e8-00000aacb35e&acdnat=1455228938_33d4226549c6410971ced1c4c3573a44)  
529 [00000aacb35e&acdnat=1455228938\\_33d4226549c6410971ced1c4c3573a44](http://ac.els-cdn.com/0042682291907595/1-s2.0-0042682291907595-main.pdf?_tid=8f811f10-d10c-11e5-82e8-00000aacb35e&acdnat=1455228938_33d4226549c6410971ced1c4c3573a44). [Accessed:  
530 11-Feb-2016].
- 531 [20] M. Husain, “HIV-1 Nef Induces Proliferation and Anchorage-Independent Growth in  
532 Podocytes,” *J. Am. Soc. Nephrol.*, vol. 13, no. 7, pp. 1806–1815, 2002, doi:  
533 10.1097/01.ASN.0000019642.55998.69.
- 534 [21] H. Li *et al.*, “Epigenetic regulation of RCAN1 expression in kidney disease and its role in  
535 podocyte injury,” *Kidney Int.*, vol. 94, no. 6, pp. 1160–1176, 2018, doi:  
536 10.1016/j.kint.2018.07.023.
- 537 [22] S. Curreli *et al.*, “B cell lymphoma in HIV transgenic mice.,” *Retrovirology*, vol. 10, p.  
538 92, Jan. 2013, doi: 10.1186/1742-4690-10-92.

- 539 [23] H. Li, “Minimap2: pairwise alignment for nucleotide sequences,” *Bioinformatics*, vol. 34,  
540 no. 18, pp. 3094–3100, May 2018, doi: 10.1093/bioinformatics/bty191.
- 541 [24] H. Li and R. Durbin, “Fast and accurate long-read alignment with Burrows – Wheeler  
542 transform,” vol. 26, no. 5, pp. 589–595, 2010, doi: 10.1093/bioinformatics/btp698.
- 543 [25] E. Afgan *et al.*, “The Galaxy platform for accessible, reproducible and collaborative  
544 biomedical analyses: 2016 update,” *Nucleic Acids Res.*, vol. 44, no. W1, pp. W3–W10,  
545 2016, doi: 10.1093/nar/gkw343.
- 546 [26] J. T. Robinson *et al.*, “Integrative genomics viewer,” *Nat Biotechnol*, vol. 29, no. 1, pp.  
547 24–26, 2011, doi: 10.1038/nbt0111-24.
- 548 [27] B. P. Walenz, S. Koren, N. H. Bergman, A. M. Phillippy, J. R. Miller, and K. Berlin,  
549 “Canu: scalable and accurate long-read assembly via adaptive k -mer weighting and repeat  
550 separation,” *Genome Res.*, vol. 27, no. 5, pp. 722–736, 2017, doi: 10.1101/gr.215087.116.
- 551 [28] S. Andrews, “FastQC A Quality Control tool for High Throughput Sequence Data.”
- 552 [29] K. Katoh and D. M. Standley, “MAFFT multiple sequence alignment software version 7:  
553 Improvements in performance and usability,” *Mol. Biol. Evol.*, vol. 30, no. 4, pp. 772–780,  
554 2013, doi: 10.1093/molbev/mst010.
- 555 [30] K. Katoh, J. Rozewicki, and K. D. Yamada, “MAFFT online service: multiple sequence  
556 alignment, interactive sequence choice and visualization,” *Brief. Bioinform.*, vol. 20, no. 4,  
557 pp. 1160–1166, Sep. 2017, doi: 10.1093/bib/bbx108.
- 558 [31] D. M. Lyons and A. S. Lauring, “Evidence for the Selective Basis of Transition-to-  
559 Transversion Substitution Bias in Two RNA Viruses,” *Mol. Biol. Evol.*, vol. 34, no. 12,  
560 pp. 3205–3215, 2017, doi: 10.1093/molbev/msx251.
- 561 [32] N. J. Loman, J. Quick, and J. T. Simpson, “A complete bacterial genome assembled de



- 562 novo using only nanopore sequencing data,” *Nat. Methods*, vol. 12, no. 8, pp. 733–735,  
563 2015, doi: 10.1038/nmeth.3444.
- 564 [33] A. Gener *et al.*, “PEA0011 - Insights from HIV-1 transgene insertions in the murine  
565 model of HIV-associated nephropathy,” in *23rd International AIDS Conference*  
566 (*AIDS2020*), 2020, vol. ePoster.
- 567 [34] A. R. Gener *et al.*, “P39 - Insights from comprehensive transcript models of HIV-1,” in  
568 *Genome Informatics 2020*, 2020, p. ePoster.
- 569 [35] A. R. Gener, T. Washington, D. Hyink, and P. Klotman, “3264 - The Multiple HIV-1  
570 Transgenes in the Murine Model of HIV-Associated Nephropathy Fail to Segregate as  
571 Expected,” in *American Society of Human Genetics Annual Meeting*, 2020, p. ePoster.
- 572 [36] A. Payne, N. Holmes, V. Rakyan, and M. Loose, “Whale watching with BulkVis: A  
573 graphical viewer for Oxford Nanopore bulk fast5 files,” *bioRxiv*, p. 312256, Jan. 2018,  
574 doi: 10.1101/312256.
- 575 [37] P. Rosenstiel, A. Gharavi, V. D’Agati, and P. Klotman, “Transgenic and infectious animal  
576 models of HIV-associated nephropathy,” *J. Am. Soc. Nephrol.*, vol. 20, no. 11, pp. 2296–  
577 304, 2009, doi: 10.1681/ASN.2008121230.
- 578 [38] M. Kvaratskhelia, A. Sharma, R. C. Larue, E. Serrao, and A. Engelman, “Molecular  
579 mechanisms of retroviral integration site selection,” *Nucleic Acids Res.*, vol. 42, no. 16,  
580 pp. gku769-, 2014, doi: 10.1093/nar/gku769.
- 581 [39] B. Marini *et al.*, “Nuclear architecture dictates HIV-1 integration site selection,” *Nature*,  
582 vol. 521, pp. 227–233, 2015, doi: 10.1038/nature14226.
- 583 [40] H. Ochman, A. S. Gerber, and D. L. Hartl, “Genetic applications of an inverse polymerase  
584 chain reaction,” *Genetics*, vol. 120, no. 3, pp. 621–623, 1988.

- 585 [41] W.-S. Hu and S. H. Hughes, “HIV-1 Reverse Transcription,” *Cold Spring Harb. Perspect.*  
586 *Med.* , vol. 2, no. 10, Oct. 2012, doi: 10.1101/cshperspect.a006882.
- 587 [42] M. R. Green, T. Maniatis, and D. A. Melton, “Human beta-globin pre-mRNA synthesized  
588 in vitro is accurately spliced in *Xenopus* oocyte nuclei.,” *Cell*, vol. 32, no. 3, pp. 681–  
589 694, Mar. 1983, doi: 10.1016/0092-8674(83)90054-5.
- 590 [43] A. R. Gener, “Full-coverage sequencing of HIV-1 provirus from a reference plasmid,”  
591 *bioRxiv*, p. 611848, Jan. 2019, doi: 10.1101/611848.
- 592 [44] B. Lucic *et al.*, “Spatially clustered loci with multiple enhancers are frequent targets of  
593 HIV-1,” *bioRxiv*, 2018.
- 594 [45] W. J. Kent *et al.*, “The Human Genome Browser at UCSC,” *Genome Res.* , vol. 12, no. 6,  
595 pp. 996–1006, Jun. 2002, doi: 10.1101/gr.229102.
- 596 [46] Y. Peng, H. C. M. Leung, S. M. Yiu, and F. Y. L. Chin, “IDBA – A Practical Iterative de  
597 Bruijn Graph De Novo Assembler BT - Research in Computational Molecular Biology,”  
598 2010, pp. 426–440.
- 599 [47] P. J. A. Cock, B. A. Grüning, K. Paszkiewicz, and L. Pritchard, “Galaxy tools and  
600 workflows for sequence analysis with applications in molecular plant pathology,” *PeerJ*,  
601 vol. 1, p. e167, 2013, doi: 10.7717/peerj.167.
- 602 [48] C. B, W. T, and S. S, “Genome sequence assembly using trace signals and additional  
603 sequence information.,” *Comput. Sci. Biol. Proc. Ger. Conf. Bioinforma.*, vol. 99, pp. 45–  
604 56.
- 605 [49] A. Bankevich *et al.*, “SPAdes: A New Genome Assembly Algorithm and Its Applications  
606 to Single-Cell Sequencing,” *J. Comput. Biol.*, vol. 19, no. 5, pp. 455–477, Apr. 2012, doi:  
607 10.1089/cmb.2012.0021.

- 608 [50] G. Cuccuru *et al.*, “Orione, a web-based framework for NGS analysis in microbiology,”  
609 *Bioinformatics*, vol. 30, no. 13, pp. 1928–1929, Jul. 2014, doi:  
610 10.1093/bioinformatics/btu135.
- 611 [51] R. L. Warren, G. G. Sutton, S. J. M. Jones, and R. A. Holt, “Assembling millions of short  
612 DNA sequences using SSAKE,” *Bioinformatics*, vol. 23, no. 4, pp. 500–501, Feb. 2007,  
613 doi: 10.1093/bioinformatics/btl629.
- 614
- 615

616 **Tables**

617

618 **Table 1: Summary of pHXB2 sample divergence from reference HXB2.**

Site	Position	Change	Substitution Class	Change	Mutation Class (Syn/Non/Stop)	Homopolymer-adjacent?	Same as neighbor?	LANL Feature	Subfeature	Frame
1	24	C>A	transversion	NA	NA	yes	yes	5'LTR	U3	NA
2	108	A>G	transition	NA	NA	yes	yes	5'LTR	U3	NA
3	164	G>T	transversion	NA	NA	yes	no	5'LTR	U3	NA
4	168	T>G	transversion	NA	NA	yes	yes	5'LTR	U3	NA
5	176	A>G	transition	NA	NA	yes	yes	5'LTR	U3	NA
6	182	C>T	transition	NA	NA	yes	no	5'LTR	U3	NA
7	227	A>G	transition	NA	NA	yes	yes	5'LTR	U3	NA
8	291	A>G	transition	NA	NA	no	no	5'LTR	U3	NA
9	333	C>T	transition	NA	NA	no	no	5'LTR	U3	NA
10	654	C>T	transition	NA	NA	no	no	None	None	NA
11	1659	aaG>aaA	transition	None	Syn	yes	yes	gag	p24, p55	gag frame 1
12	2259	gag:agG>agA pol:Gtc>Atc	transition	gag:Arg>Arg pol:Val>Ile	Syn/Non	no	no	gagpol	p6	gag frame 1 pol frame 3
13	2927	aaG>aaA	transition	None	Syn	yes	yes	pol	p51 RT	pol frame 3
14	3812	ccC>ccT	transition	None	Syn	yes	yes	pol	p51 RT	pol frame 3
15	4574	acT>acA	transversion	None	Syn	no	no	pol	p31 IN	pol frame 3
16	4596	Ggt>Agt	transition	None	Syn	yes	no	pol	p31 IN	pol frame 3
17	4609	aGg>aAg	transition	Arg>Lys	Non	yes	yes	pol	p31 IN	pol frame 3
18	7823	gcC>gcG Ggc>Cgc	transversion	ASP:Gly>Arg	Syn/Non	no	no	gp41	RRE, also ASP	gp41 frame 3, ASP -2
19	9253	Ata>Gta	transition	Ile>val	Non	no	yes	nef/3'LTR	also U3	nef frame 1
20	9418	C>T	transition	NA	NA	no	no	3'LTR	U3	NA

619 Coverage numbers vary by input (albacore, guppy, FlipFlop basecalled FASTQ) and mapping  
620 method (Minimap2 vs. BWA-MEM). This information is provided as Supplemental Digital

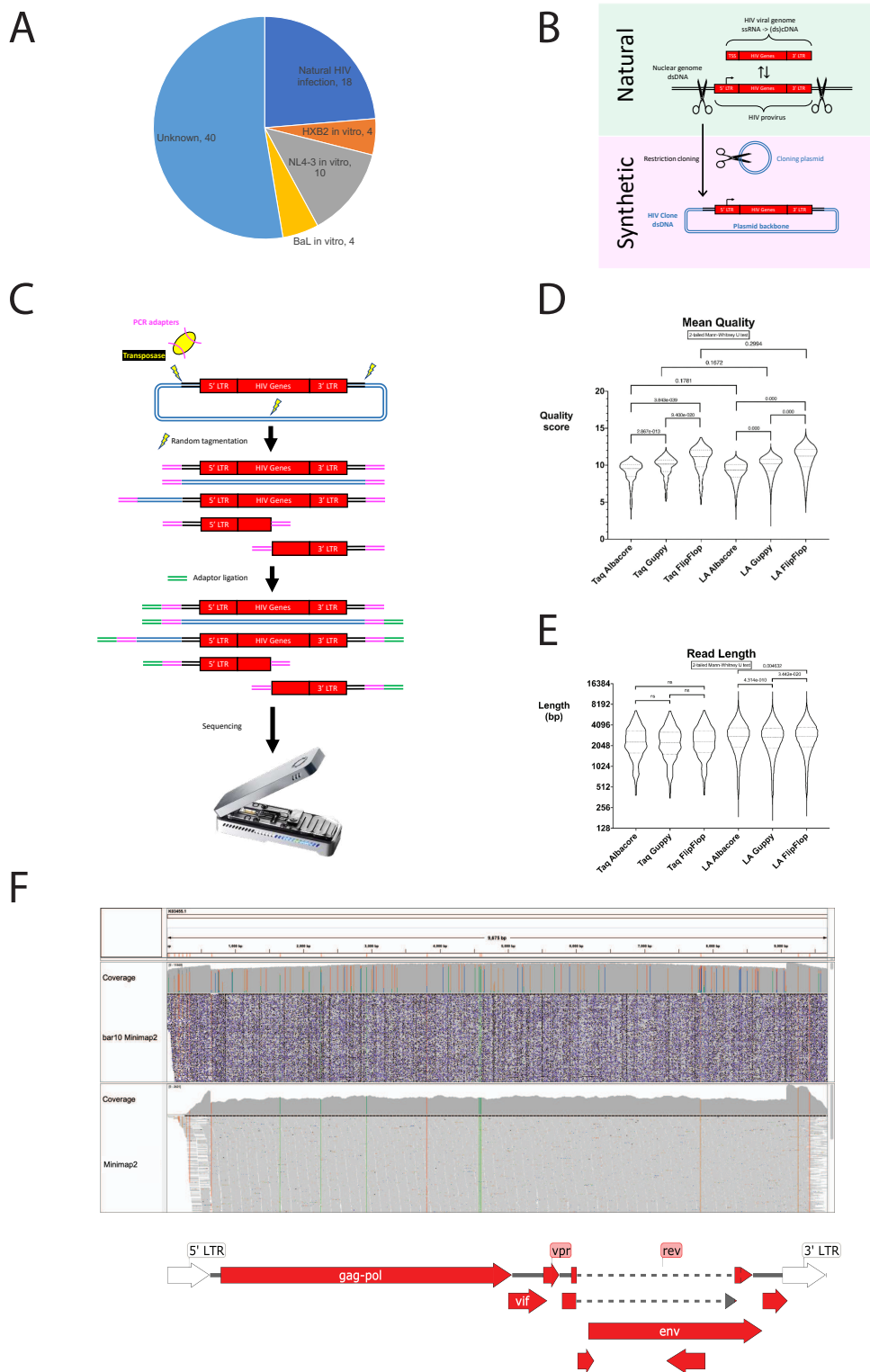
621 Content. Base-1 (first base is numbered 1, 2<sup>nd</sup> 2, etc.), relative to HXB2, Genbank:K03455.1.  
622 Changed base represented as upper-case. Annotated as codon if in protein-coding region. No  
623 deletions or insertions were predicted from manual inspection or supported by short-read  
624 sequencing. Abbreviations, ASP: antisense protein, RRE: rev-response element, NA: not  
625 applicable. Syn: synonymous mutation. Non: non-synonymous mutation. Stop: stop codon/non-  
626 sense mutation. LTR: long terminal repeat. RT: reverse transcriptase. IN: integrase. LANL: Los  
627 Alamos National Laboratory HIV Sequence Database. Data from three separate sequencing  
628 experiments on the same plasmid sample support these 20 sites. Note site 1-8 variants in 5'LTR  
629 have been previously reported (LANL), albethey ambiguously. These may also be incorrectly  
630 annotated as variants in nef.

631 **Figures**

632

633

634 **Figure 1: HIV information in pHXB2\_D is recovered by long-read sequencing and**  
 635 **mapping.**





637 Figure 1A: HXB2 is still a commonly used resource. It is the reference HIV-1 genome, derived  
638 from one of the earliest clinical isolates. While older HIV samples are occasionally rediscovered,  
639 they are not made routinely available to researchers. All public HIV-1 RNA-seq datasets were  
640 obtained from the NCBI SRA with the following search phrase: “HIV-1” AND “RNA-seq”.  
641 Metadata from these 2527 runs (number current as of 7/21/2020) were used to make a pie chart  
642 summary.

643 Figure 1B: HIV information comes from three main sources: proviruses (HIV sandwiched  
644 between two assumedly identical full-length long terminal repeats (LTRs)), unspliced HIV  
645 mRNAs (also known as viral genomes) starting from the transcription start site and ending in the  
646 3’ LTR [4], and engineered proviruses recovered in their entirety or stitched together from  
647 multiple isolates like NL4-3 [18].

648 Figure 1C: ONT library prep pipeline. Tagmentation cleaves double-stranded DNA, ligating  
649 barcoded PCR adapters (magenta). PCR-adapted DNA may be amplified. After amplification  
650 and cleanup, ONT sequencing adapters (green) are ligated. Barcoded samples may be pooled and  
651 sequenced.

652 Figure 1D: Newer basecallers increase read mean quality. Median (big dash) and quartiles (little  
653 dash). Effect of enzyme version was not statistically significant.

654 Figure 1E: Read stats with different callers/aligners. Median (big dash) and quartiles (little dash).  
655 Read lengths increase with higher fidelity Taq.

656 Figure 1F: Sequencing coverage with long- vs. short-read single-end 150 bp (trimmed to 142 bp)  
657 DNA sequencing. Long-read sequencing covers ambiguously mappable areas missed by short-  
658 read in HXB2 reference Genbank:K03455.1 (**Supplemental Figures 3D,3E**), but at the expense  
659 of accuracy near homopolymers longer than about 4 nucleobases (**Supplemental Figure 5**).

660 Short-read mapping fails at repetitive elements longer than their read lengths (**Supplemental**  
661 **Figures 3D,3E**). Long read Minimap2 settings: map-ont -k15. Short read Minimap2 settings:  
662 Short reads without splicing (-k21 -w11 --sr -F800 -A2 -B8 -O12,32 -E2,1 -r50 -p.5 -N20 -  
663 f1000,5000 -n2 -m20 -s40 -g200 -2K50m --heap-sort=yes --secondary=no) (sr).  
664  
665  
666



669 The 5<sup>th</sup> longest read in the barcode 10 set (read ID 6fbf0205-5195-460e-8e28-930db50e5d79)  
670 contained full-length HIV-1. Query (full read) blastn against HIV (taxid:11676) returned 92.95%  
671 identity to HIV-1, complete genome (Genbank:AF033819.3). Limiting query to HXB2 (red)  
672 blastn against Nucleotide collection nr/nt returned 100% coverage and 93.02% identity to HIV-1  
673 HXB2. This read was 11,487 bases long, with mean quality score 11.984396. Basecalled using  
674 Guppy 2.3.1 with FlipFlop config.  
675

676 **Figure 3A: pHXB2\_D has identical LTRs, resolving likely errors in HXB2 (K03455.1)**

```

677 CLUSTAL format alignment by MAFFT (v7.475)
678
679
680 K03455.1_5'LTR   tggaagggctaattcactcccaacgaagacaagatatccttgatctgtggatctaccaca
681 pHXB2_D_5'LTR   tggaagggctaattcactcccaagaagacaagatatccttgatctgtggatctaccaca
682 pHXB2_D_3'LTR   tggaagggctaattcactcccaagaagacaagatatccttgatctgtggatctaccaca
683 K03455.1_3'LTR   tggaagggctaattcactcccaagaagacaagatatccttgatctgtggatctaccaca
684
685 *****
686 K03455.1_5'LTR   cacaaggctacttccctgattagcagaactacacaccagggccagggatcagatatccac
687 pHXB2_D_5'LTR   cacaaggctacttccctgattagcagaactacacaccagggccaggggtcagatatccac
688 pHXB2_D_3'LTR   cacaaggctacttccctgattagcagaactacacaccagggccaggggtcagatatccac
689 K03455.1_3'LTR   cacaaggctacttccctgattagcagaactacacaccagggccaggggtcagatatccac
690
691 *****
692 K03455.1_5'LTR   tgacctttggatggtgctacaagctagtaccagttgagccagagaaggtagaagaagcca
693 pHXB2_D_5'LTR   tgacctttggatggtgctacaagctagtaccagttgagccagataaggtagaagaggcca
694 pHXB2_D_3'LTR   tgacctttggatggtgctacaagctagtaccagttgagccagataaggtagaagaggcca
695 K03455.1_3'LTR   tgacctttggatggtgctacaagctagtaccagttgagccagataagatagaagaggcca
696
697 *****
698 K03455.1_5'LTR   acaaaggagagaacaccagcttgttacaccctgtgagcctgcatggaatggatgaccgg
699 pHXB2_D_5'LTR   ataaaggagagaacaccagcttgttacaccctgtgagcctgcatgggatggatgaccgg
700 pHXB2_D_3'LTR   ataaaggagagaacaccagcttgttacaccctgtgagcctgcatgggatggatgaccgg
701 K03455.1_3'LTR   ataaaggagagaacaccagcttgttacaccctgtgagcctgcatgggatggatgaccgg
702
703 *.....
704 K03455.1_5'LTR   agagagaagtgttagagtggaggtttgacagccgcctagcatttcatcacatggcccag
705 pHXB2_D_5'LTR   agagagaagtgttagagtggaggtttgacagccgcctagcatttcatcacatggcccag
706 pHXB2_D_3'LTR   agagagaagtgttagagtggaggtttgacagccgcctagcatttcatcacatggcccag
707 K03455.1_3'LTR   agagagaagtgttagagtggaggtttgacagccgcctagcatttcatcacatggcccag
708
709 *****
710 K03455.1_5'LTR   agctgcatccggagtacttcaagaactgctgacatcgagcttgctacaagggactttccg
711 pHXB2_D_5'LTR   agctgcatccggagtacttcaagaactgctgatatcgagcttgctacaagggactttccg
712 pHXB2_D_3'LTR   agctgcatccggagtacttcaagaactgctgatatcgagcttgctacaagggactttccg
713 K03455.1_3'LTR   agctgcatccggagtacttcaagaactgctgacatcgagcttgctacaagggactttccg
714
715 *****
716 K03455.1_5'LTR   ctggggactttccagggaggcgtggcctgggaggactggggagtgggcgagccctcagat

```

```
717 pHXB2_D_5'LTR ctggggactttccagggagggcgtggcctgggcgggactggggagtggcgagccctcagat
718 pHXB2_D_3'LTR ctggggactttccagggagggcgtggcctgggcgggactggggagtggcgagccctcagat
719 K03455.1_3'LTR ctggggactttccagggagggcgtggcctgggcgggactggggagtggcgagccctcagat
720 *****
721
722 K03455.1_5'LTR cctgcatataagcagctgctttttgcctgtactgggtctctctgggttagaccagatctga
723 pHXB2_D_5'LTR cctgcatataagcagctgctttttgcctgtactgggtctctctgggttagaccagatctga
724 pHXB2_D_3'LTR cctgcatataagcagctgctttttgcctgtactgggtctctctgggttagaccagatctga
725 K03455.1_3'LTR cctgcatataagcagctgctttttgcctgtactgggtctctctgggttagaccagatctga
726 *****
727
728 K03455.1_5'LTR gcctgggagctctctgggctaactaggggaaccactgcttaagcctcaataaagcttgccct
729 pHXB2_D_5'LTR gcctgggagctctctgggctaactaggggaaccactgcttaagcctcaataaagcttgccct
730 pHXB2_D_3'LTR gcctgggagctctctgggctaactaggggaaccactgcttaagcctcaataaagcttgccct
731 K03455.1_3'LTR gcctgggagctctctgggctaactaggggaaccactgcttaagcctcaataaagcttgccct
732 *****
733
734 K03455.1_5'LTR tgagtgcttcaagtagtgtgtgcccgtctgttggtgtgactctggtaactagagatccctc
735 pHXB2_D_5'LTR tgagtgcttcaagtagtgtgtgcccgtctgttggtgtgactctggtaactagagatccctc
736 pHXB2_D_3'LTR tgagtgcttcaagtagtgtgtgcccgtctgttggtgtgactctggtaactagagatccctc
737 K03455.1_3'LTR tgagtgcttcaagtagtgtgtgcccgtctgttggtgtgactctggtaactagagatccctc
738 *****
739
740 K03455.1_5'LTR agacccttttagtcagtggtggaaaatctctagca
741 pHXB2_D_5'LTR agacccttttagtcagtggtggaaaatctctagca
742 pHXB2_D_3'LTR agacccttttagtcagtggtggaaaatctctagca
743 K03455.1_3'LTR agacccttttagtcagtggtggaaaatctctagca
744 *****
```

745

746

747 **Figure 3B: pNL4-3\_gag-pol( $\Delta$ 1443-4553)\_EGFP (ACCESSION\_TBD) has distinct LTRs,**  
 748 **consistent with pNL4-3 (AF324493.1)**

```

749 CLUSTAL format alignment by MAFFT (v7.475)
750
751
752 AF324493.1_5LTR  tggaagggctaatttgggtcccaaaaaagacaagagatccttgatctgtggatctaccaca
753 ACCESSION_TBD_5  tggaagggctaatttgggtcccaaaaaagacaagagatccttgatctgtggatctaccaca
754 AF324493.1_3LTR  tggaagggctaattcactcccaagaagacaagatataccttgatctgtggatctaccaca
755 ACCESSION_TBD_3  tggaagggctaattcactcccaagaagacaagatataccttgatctgtggatctaccaca
756 *****.. *****.***** *****
757
758 AF324493.1_5LTR  cacaaggctacttccctgattggcagaactacacaccagggccagggatcagatatccac
759 ACCESSION_TBD_5  cacaaggctacttccctgattggcagaactacacaccagggccagggatcagatatccac
760 AF324493.1_3LTR  cacaaggctacttccctgattggcagaactacacaccagggccaggggtcagatatccac
761 ACCESSION_TBD_3  cacaaggctacttccctgattggcagaactacacaccagggccaggggtcagatatccac
762 *****.*****
763
764 AF324493.1_5LTR  tgacctttggatggtgcttcaagttagtaccagttgaaccagagcaagtagaagaggcca
765 ACCESSION_TBD_5  tgacctttggatggtgcttcaagttagtaccagttgaaccagagcaagtagaagaggcca
766 AF324493.1_3LTR  tgacctttggatggtgctacaagctagtaccagttgagccagataaggtagaagaggcca
767 ACCESSION_TBD_3  tgacctttggatggtgctacaagctagtaccagttgagccagataaggtagaagaggcca
768 ***** ****.*****.***** *.*****
769
770 AF324493.1_5LTR  atgaaggagagaacaacagcttgttacaccctatgagccagcatgggatggaggaccg
771 ACCESSION_TBD_5  atgaaggagagaacaacagcttgttacaccctatgagccagcatgggatggaggaccg
772 AF324493.1_3LTR  ataaaggagagaacaccagcttgttacaccctgtgagcctgcatggaatggatgaccctg
773 ACCESSION_TBD_3  ataaaggagagaacaccagcttgttacaccctgtgagcctgcatggaatggatgaccctg
774 **..***** *****.***** *****.***** ***** *
775
776 AF324493.1_5LTR  agggagaagtattagtgtggaagtttgacagcctcctagcatttcgtcacatggcccag
777 ACCESSION_TBD_5  agggagaagtattagtgtggaagtttgacagcctcctagcatttcgtcacatggcccag
778 AF324493.1_3LTR  agagagaagtgttagagtggaggttgacagccgcctagcatttcacacgtggcccag
779 ACCESSION_TBD_3  agagagaagtgttagagtggaggttgacagccgcctagcatttcacacgtggcccag
780 **..*****.***** *****.***** *****.***** *****
781
782 AF324493.1_5LTR  agctgcatccggagtactacaaagactgctgacatcgagctttctacaagggactttccg
783 ACCESSION_TBD_5  agctgcatccggagtactacaaagactgctgacatcgagctttctacaagggactttccg
784 AF324493.1_3LTR  agctgcatccggagtacttcaagaactgctgacatcgagcttgctacaagggactttccg
785 ACCESSION_TBD_3  agctgcatccggagtacttcaagaactgctgacatcgagcttgctacaagggactttccg
786 ***** ***..***** *****

```

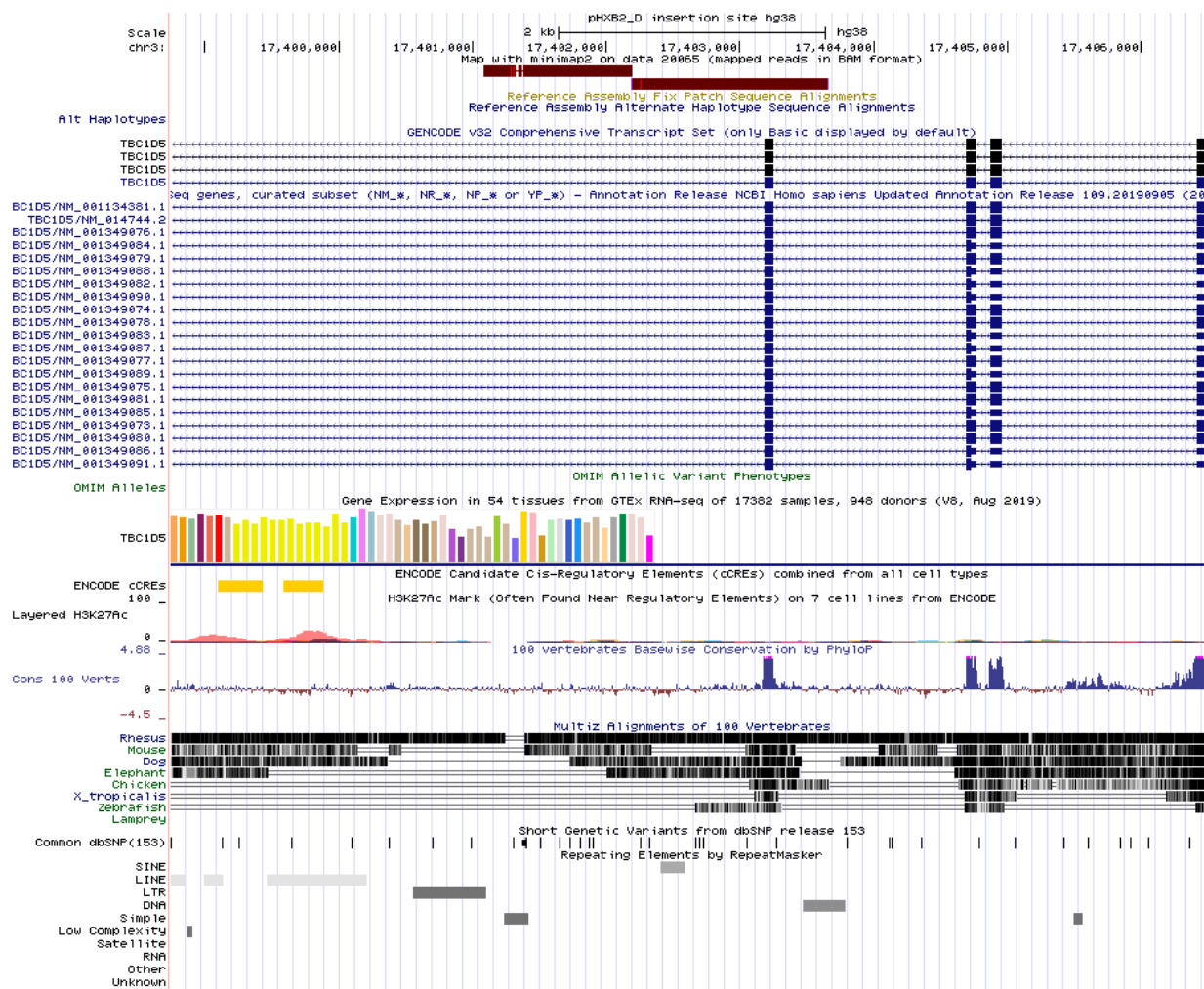
787  
788 AF324493.1\_5LTR ctggggactttccagggaggtgtggcctgggcgggactggggagtggcgagccctcagat  
789 ACCESSION\_TBD\_5 ctggggactttccagggaggtgtggcctgggcgggactggggagtggcgagccctcagat  
790 AF324493.1\_3LTR ctggggactttccagggagggcgtggcctgggcgggactggggagtggcgagccctcagat  
791 ACCESSION\_TBD\_3 ctggggactttccagggagggcgtggcctgggcgggactggggagtggcgagccctcagat  
792 \*\*\*\*\*.  
793  
794 AF324493.1\_5LTR gctacatataagcagctgctttttgcctgtactgggtctctctggtttagaccagatctga  
795 ACCESSION\_TBD\_5 gctacatataagcagctgctttttgcctgtactgggtctctctggtttagaccagatctga  
796 AF324493.1\_3LTR gctgcatataagcagctgctttttgcctgtactgggtctctctggtttagaccagatctga  
797 ACCESSION\_TBD\_3 gctgcatataagcagctgctttttgcctgtactgggtctctctggtttagaccagatctga  
798 \*\*\*.  
799  
800 AF324493.1\_5LTR gcctgggagctctctgggctaactaggggaaccactgcttaagcctcaataaagcttgct  
801 ACCESSION\_TBD\_5 gcctgggagctctctgggctaactaggggaaccactgcttaagcctcaataaagcttgct  
802 AF324493.1\_3LTR gcctgggagctctctgggctaactaggggaaccactgcttaagcctcaataaagcttgct  
803 ACCESSION\_TBD\_3 gcctgggagctctctgggctaactaggggaaccactgcttaagcctcaataaagcttgct  
804 \*\*\*\*\*.  
805  
806 AF324493.1\_5LTR tgagtgctcaaagtagtgtgtgcccgctctgttgtgtgactctggtaactagagatccctc  
807 ACCESSION\_TBD\_5 tgagtgctcaaagtagtgtgtgcccgctctgttgtgtgactctggtaactagagatccctc  
808 AF324493.1\_3LTR tgagtgcttcaagtagtgtgtgcccgctctgttgtgtgactctggtaactagagatccctc  
809 ACCESSION\_TBD\_3 tgagtgcttcaagtagtgtgtgcccgctctgttgtgtgactctggtaactagagatccctc  
810 \*\*\*\*\*.  
811  
812 AF324493.1\_5LTR agacccttttagtcagtggtggaaaatctctagca  
813 ACCESSION\_TBD\_5 agacccttttagtcagtggtggaaaatctctagca  
814 AF324493.1\_3LTR agacccttttagtcagtggtggaaaatctctagca  
815 ACCESSION\_TBD\_3 agacccttttagtcagtggtggaaaatctctagca  
816 \*\*\*\*\*

817



818 **Figure 4A: HXB2 integration site**

819



820

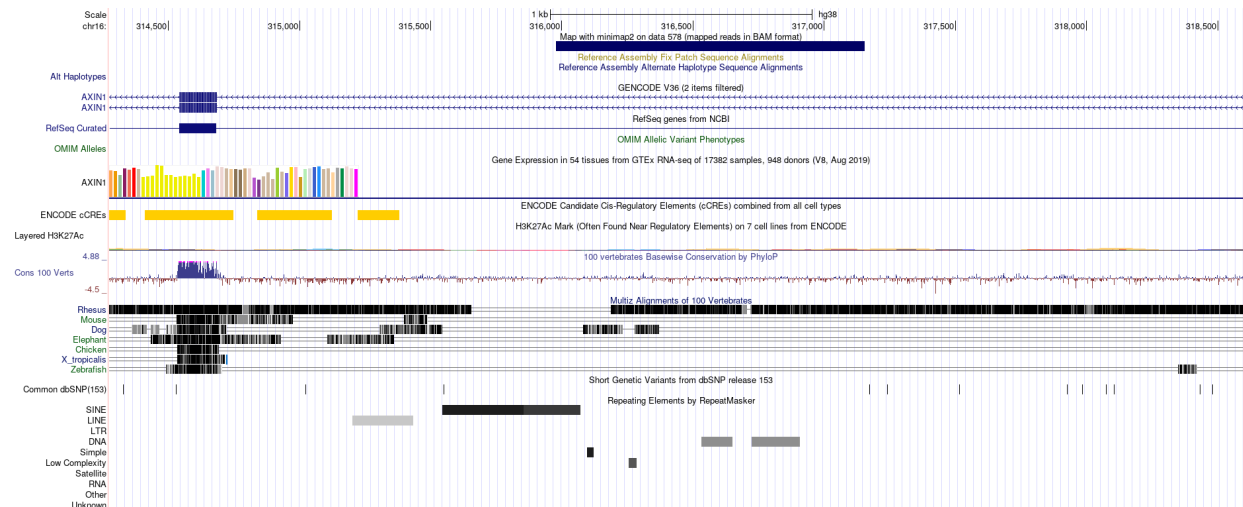
821

822

823 **Figure 4B: NL4-3 integration sites**

824

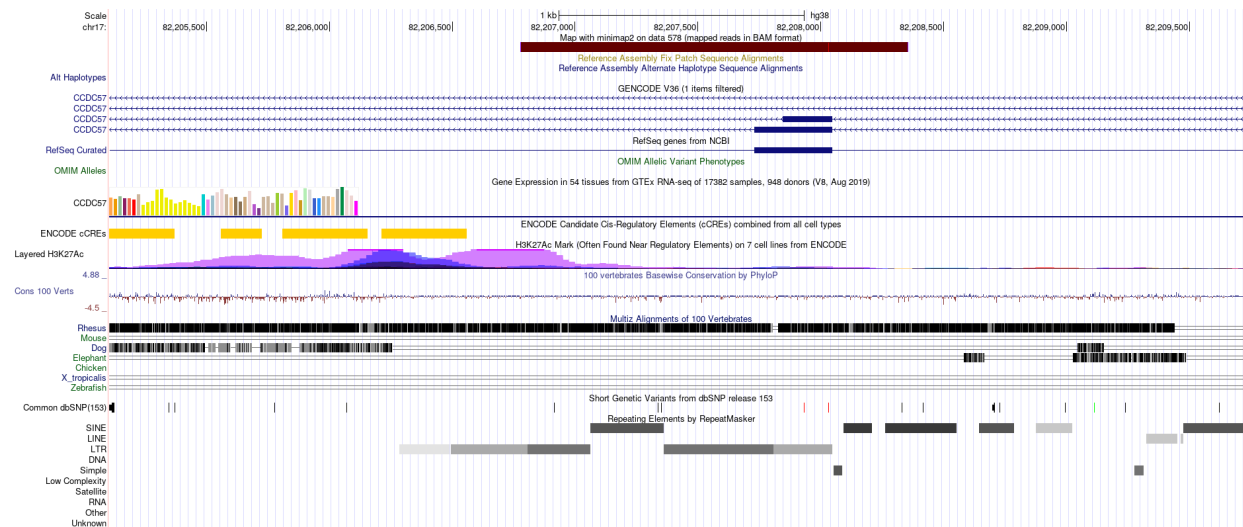
825



826

827

828



829

830

831 Figure 4A: pHXB2\_D's, and therefore HXB2's, integration site is unambiguously singular (falls  
 832 outside of annotated repeat), and in the same orientation (minus strand relative to hg38) as target  
 833 gene TBC1D5. Alignment quality is 60 for both homology arms (**Supplemental Table 2**).

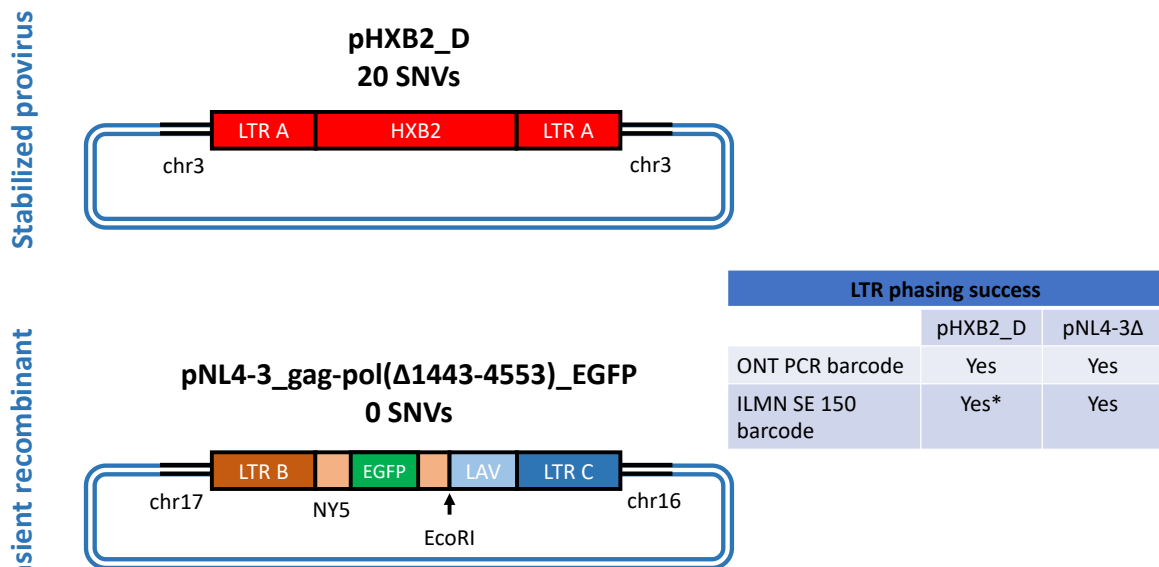
834 Features captured by homology arms in pHXB2\_D and other clones verified as proviruses in the  
 835 present study are consistent with HIV-1 integration behavior [44]. Visualized in UCSC Genome

836 Browser [45]. Figure 4B: pNL4-3\_gag-pol( $\Delta$ 1443-4553)\_EGFP's, and therefore NL4-3's,  
837 integration sites fall on annotated repeats, the longer reads help to locate both sites. Alignment  
838 quality is 60 for both homology arms (**Supplemental Table 2**). These integration sites would  
839 likely be missed by any method leveraging reads shorter than the homology arms.

840

841 **Figure 5: pHXB2\_D provenance and top 50 neighbors**

843 Figure 6: Summary of long- vs. short-read mapping by ability to phase LTRs



LTR C takes over in subsequent viruses.

\*intermittent success with ambiguous mapping at LTR.

**845 Supplemental Information**

## 846 **Data exploration with long- and short-read mapping**

847           To assemble pHXB2\_D, we tried the following short read assemblers on short-read data  
848 from the external core: IDBA [46], MIRA [47], [48], SPAdes [49], and SSAKE [50], [51]. These  
849 were chosen as a convenience because they were already stably implemented in Galaxy  
850 (specifically usegalaxy.eu). Of these, SSAKE produced discontinuous assemblies with default  
851 parameters. The discontinuous contigs did however map to the core's assembly (not shown).

## 852 **Enabling STEM outreach**

853           This work was performed as two control experiments with identically prepared libraries  
854 for a STEM outreach initiative, Student Genomics (Gener, et al., manuscript in prep). Given the  
855 constraints of the Student Genomics pilot, a rapid sequencing kit with tagmentation (explained  
856 below) with PCR barcoding was used to pool samples for ONT sequencing, with the  
857 consequence of fragmenting plasmid DNA more than what would have been ideal for capturing  
858 full-length HIV. That said, these controls could have been just as easily replaced by any  
859 samples/experiments benefiting from long-read sequencing at moderate-to-high coverage.

860

861 **Supplemental Tables**

862

863



864 **Supplemental Table 1: HXB2 is still a common HIV clone.**

865 **See Supplemental Digital Content.**

866 **See also Figure 1A.**

867

868

869

870 **Supplemental Table 2: HIV provirus clones**

871 **See Supplemental Digital Content.**

872 Of the HIV clones available through ARP, the table represents the only validated proviruses with  
873 both upstream and downstream homology arms mapping to the same integration sites. pNL4-3 is  
874 included as a known chimera with two integration half-sites. Other clones were made with  
875 cDNA cloning, usually TA cloning (per ARP entries). Note: Reference hg38. Aligner: minimap2  
876 with "Long Assembly" mapping settings. All homology arms had Alignment quality = 60.  
877 Upstream = host plus strand; independent of integration orientation. Coordinates reported from  
878 UCSC. ARP = NIH AIDS Reagent and Reference Program. IS = integration site.

879 **Supplemental Table 3: Variation in assemblies at the feature level.**

	Mismatches						Gaps (INDEL)					
	Taq			LA Taq			Taq			LA Taq		
	Albacore	Guppy	FlipFlop	Albacore	Guppy	FlipFlop	Albacore	Guppy	FlipFlop	Albacore	Guppy	FlipFlop
5' LTR	NA	9	9	9	9	9	NA	NA	0	2	0	0
gag	2	2	2	2	2	2	12	10	9	9	8	8
5' LTR+ψ	10	10	NA	NA	NA	NA	5	2	NA	NA	NA	NA
pol	7	6	6	6	6	6	26	22	9	18	11	10
vif	0	0	0	0	0	0	3	3	2	3	1	1
vpr	0	0	0	0	0	0	1	1	1	0	0	0
tat	2	1	1	1	1	1	10	6	3	7	4	5
rev	2	1	1	1	1	1	10	7	4	7	4	5
vpu	1	0	0	0	0	0	0	0	0	0	0	0
gp160	2	1	1	1	1	1	11	7	4	8	4	5
nef	1	1	1	1	1	1	3	2	2	3	2	1
3' LTR	2	2	NA	NA	NA	NA	2	0	NA	NA	NA	NA
nef+3' LTR	NA	2	2	2	2	2	NA	2	2	5	2	1
HXB2	22	20	20	20	20	20	61	46	28	47	27	25
Downstream bridge	0	0	0	0	0	0	4	5	1	2	1	1
pBR322-related	0	0	0	0	0	0	19	19	13	18	19	15
Upstream bridge	2	2	3	2	2	2	8	6	5	7	7	3

880

881 Assembled with Canu. NA denotes features which may not have matched exactly, but which

882 were collapsed with adjacent features to facilitate counting. Variants called manually by

883 mapping assemblies over HXB2 features with SnapGene.

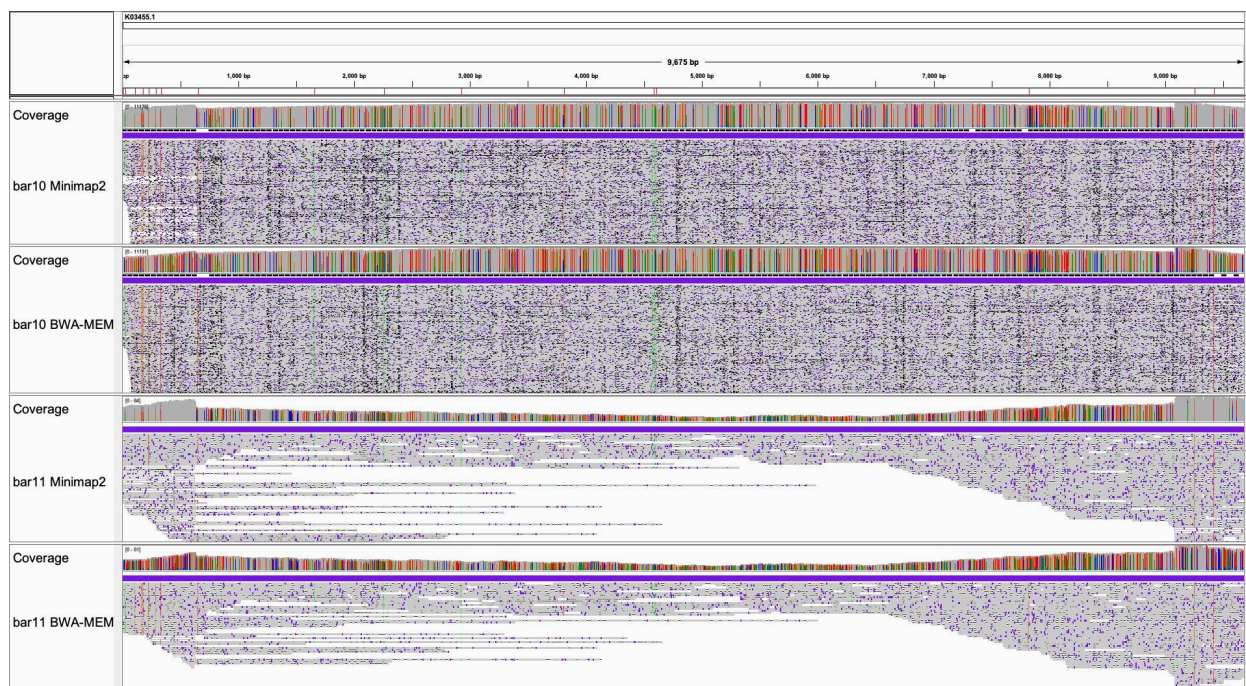
884

885

886 **Supplemental Figures**

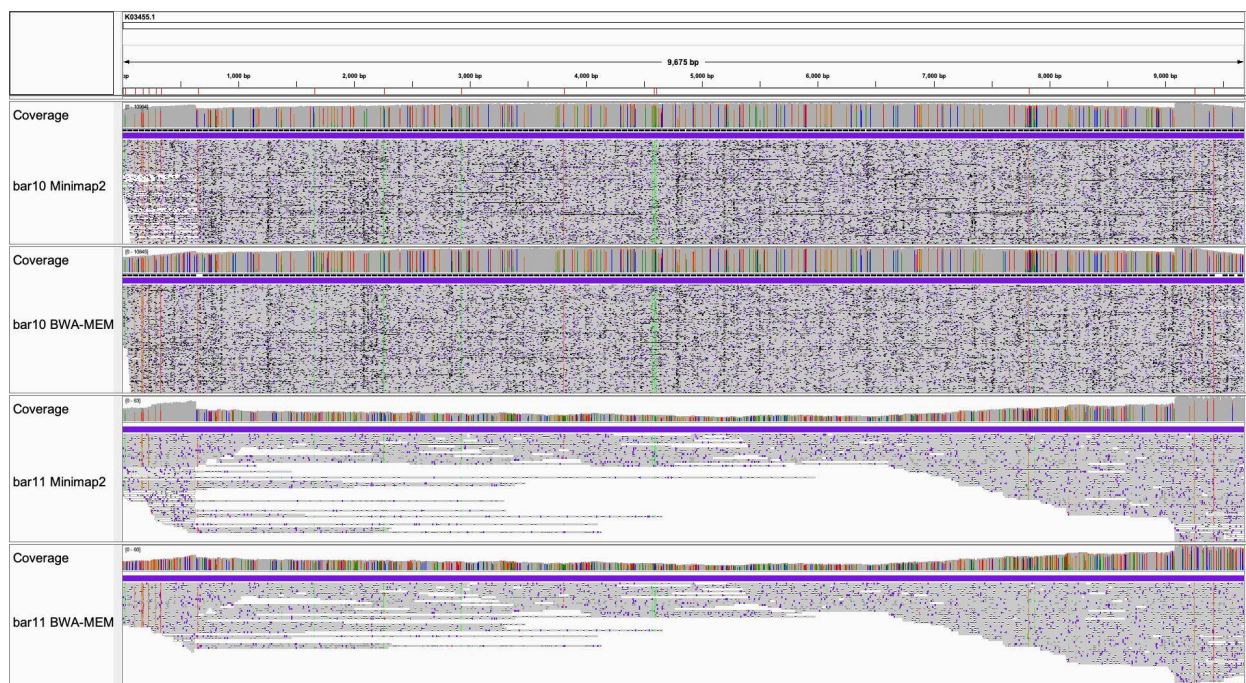
887

888 **Supplemental Figure 1A: Unbiased nanopore DNA sequencing coverage over HXB2**  
889 **depends on DNA polymerase and mapper. ONT basecaller = Albacore (worst).**



890  
891

892 **Supplemental Figure 1B: Unbiased nanopore DNA sequencing coverage over HXB2**  
893 **depends on DNA polymerase and mapper. ONT basecaller = Guppy.**



894  
895



896 **Supplemental Figure 1C: Unbiased nanopore DNA sequencing coverage over HXB2**  
897 **depends on DNA polymerase and mapper. ONT basecaller = FlipFlop (best).**



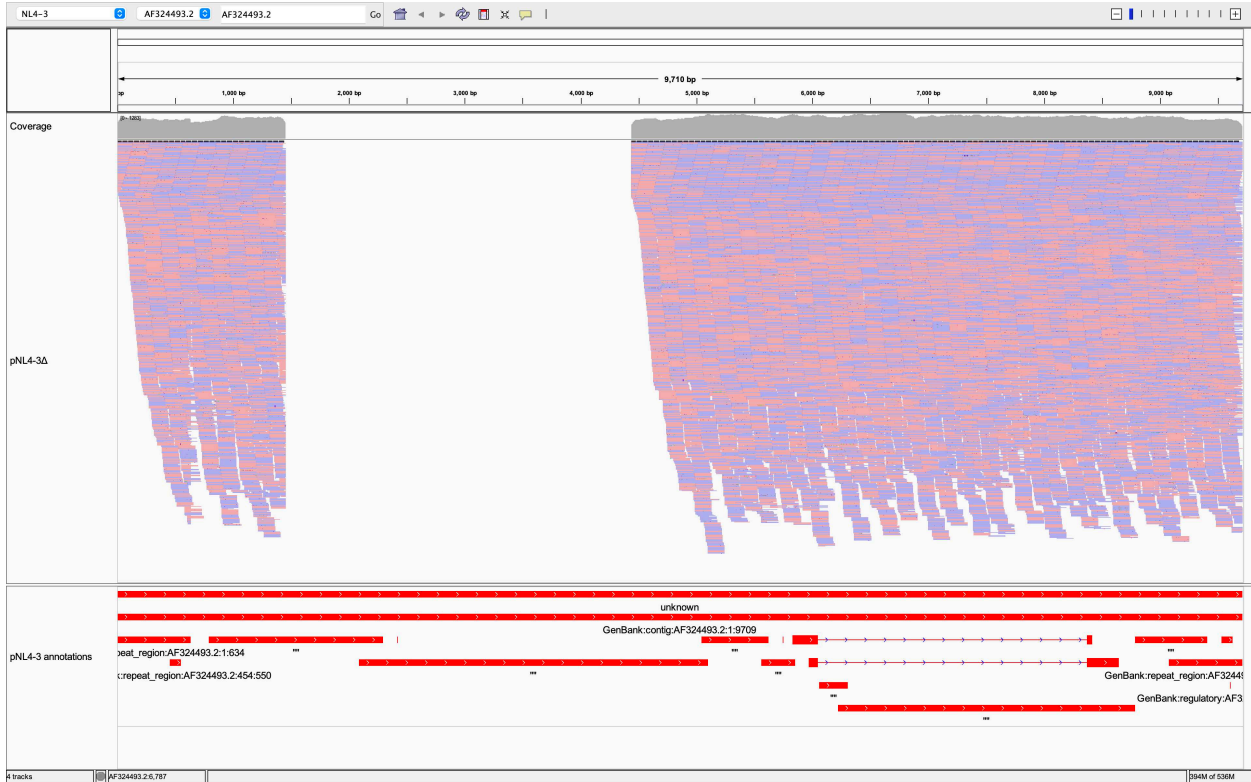
898  
899

900 Top two Coverage and Alignment panels from barcoded library 10 (bar10 = LA Taq). Bottom  
901 two from Barcode 11 (bar11 = Taq). Minimap2 and BWA-MEM were used to map reads  
902 basecalled with Albacore (worst), Guppy, or FlipFlop (best) to HXB2. Color-coding: Red below  
903 genome scale marks 20 SNVs across the HIV segment of pHXB2\_D. Purple is an insertion in a  
904 given read relative to reference. White is either a deletion in a given read or space between two  
905 aligned reads. Gray in alignment field means base same as reference, and in coverage field  
906 means major allele is at least 95% the same as reference. Per-read “insertions” and “deletions”  
907 do not necessarily represent true insertions or deletions actually present in the sample, because  
908 each read is likely an imperfect independent observation. Automated assembly followed by  
909 manual consensus building converts these overlapping reads into approximations of the ground  
910 truth. “Unbiased” refers to not amplifying a given region (e.g., pol) before ligating ONT  
911 sequencing adapters. In the present approach, the tagmentation process randomly cuts DNA,  
912 creating ~2000 bp pieces. Tagmented DNA is then amplified based on tagmentation adapters.  
913



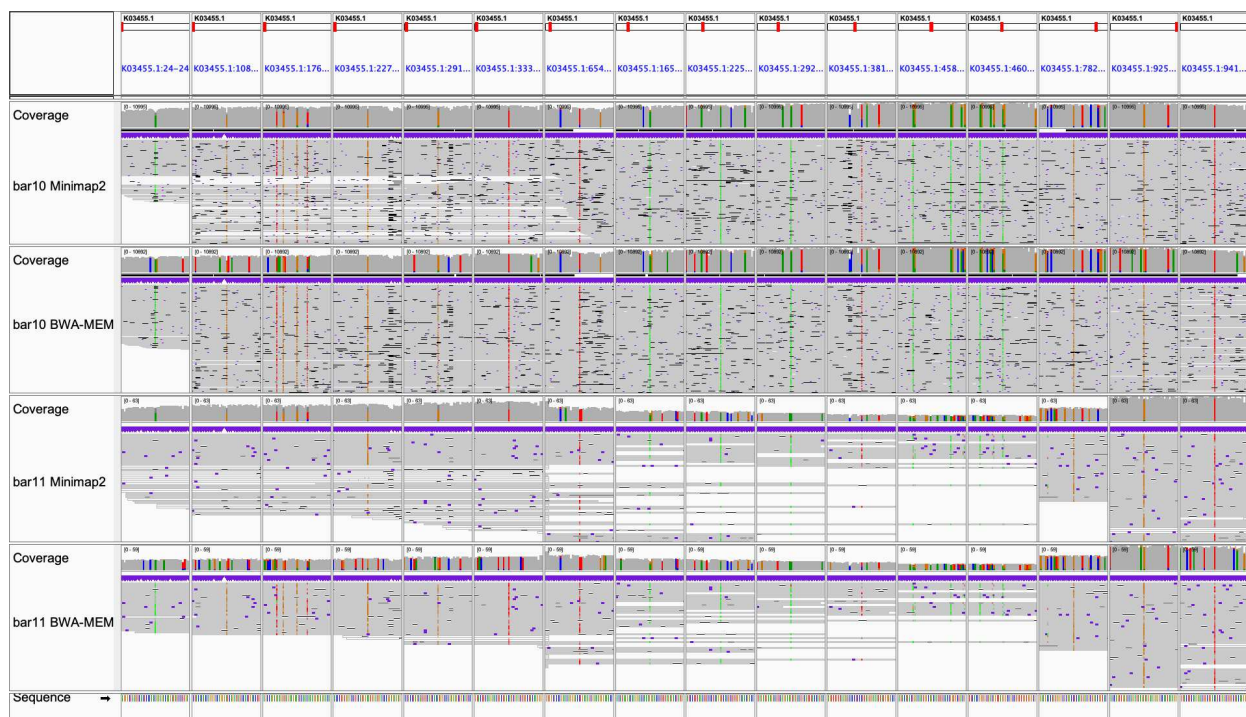
914 **Supplemental Figure 2: Reads map well to HIV-1 NL4-3 segment of pNL4-3 assembly**  
915 **because NL4-3 LTRs are distinct.**

916



917  
918

919 **Supplemental Figure 3A: HIV single nucleotide variants (SNVs) in pHXB2\_D. ONT**  
 920 **basecaller = Albacore (worst).**



921  
922

923 **Supplemental Figure 3B: HIV single nucleotide variants (SNVs) in pHXB2\_D. ONT**  
924 **basecaller = Guppy.**



925  
926

927 **Supplemental Figure 3C: HIV single nucleotide variants (SNVs) in pHXB2\_D. ONT**

928 **basecaller = FlipFlop (best).**



929  
930

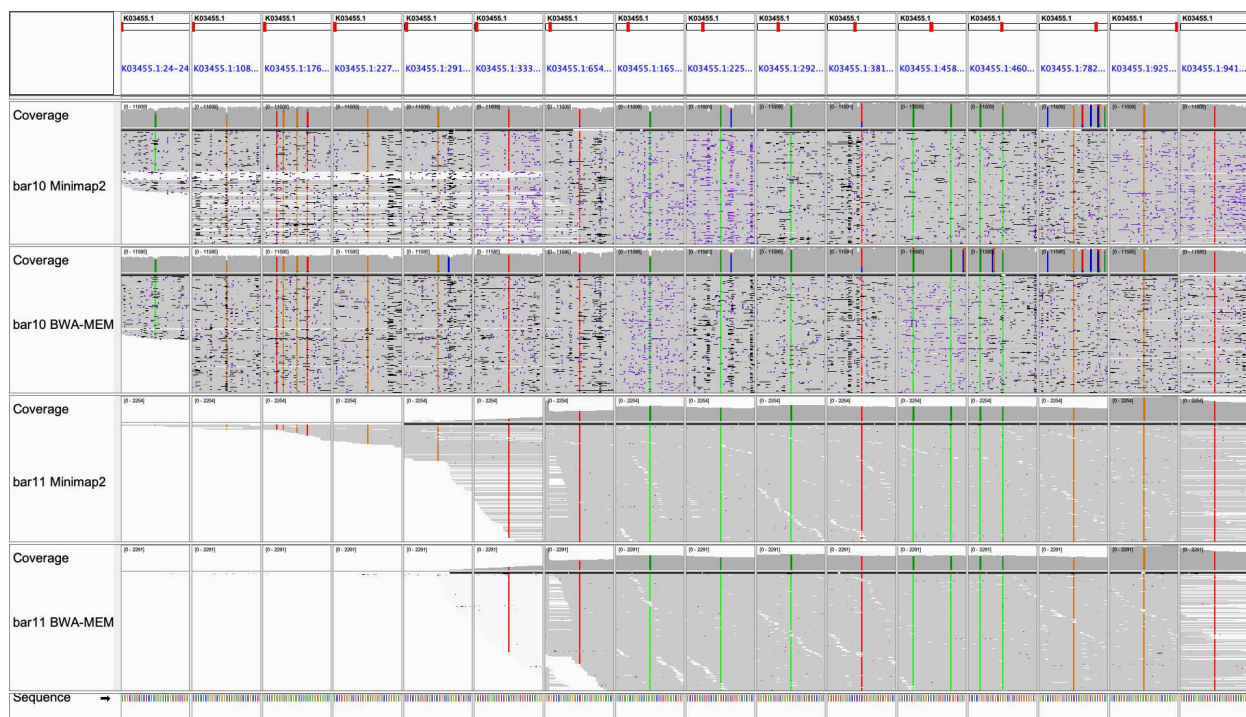


931 **Supplemental Figure 3D: HIV single nucleotide variants (SNVs) in pHXB2\_D, long vs.**  
932 **short reads (HIV genome).**



933  
934

935 Supplemental Figure 3E: HIV single nucleotide variants (SNVs) in pHXB2\_D, long vs.  
 936 short reads (20 SNV-focused).



937  
 938

939 Supplemental Figure 3A: HIV single nucleotide variants (SNVs) in pHXB2\_D. ONT basecaller  
940 = Albacore (worst). Gray indicates per-base consensus accuracy  $\geq 80\%$ . These alignments are  
941 the noisiest (less gray and most divergent from reference) between Supplemental Figures 3A,  
942 3B, and 3C.

943 Supplemental Figure 3B: HIV single nucleotide variants (SNVs) in pHXB2\_D. ONT basecaller  
944 = Guppy.

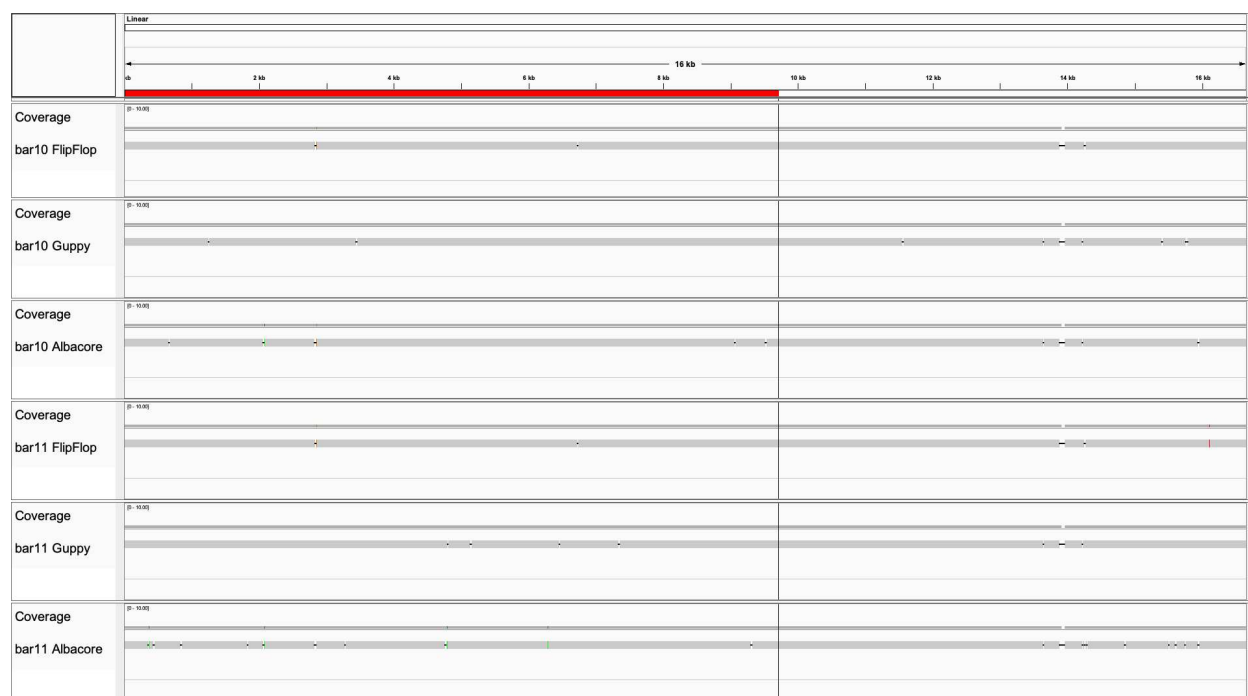
945 Supplemental Figure 3C: HIV single nucleotide variants (SNVs) in pHXB2\_D. ONT basecaller  
946 = FlipFlop (best). These alignments are the least noisy (most gray and like reference) between  
947 Supplemental Figures 3A, 3B, and 3C.

948 Supplemental Figure 3D: HIV single nucleotide variants (SNVs) in pHXB2\_D, long vs. short  
949 reads (HIV genome). Long reads outperform short reads at HIV-1 LTRs. ONT basecaller =  
950 FlipFlop. Short read as single-end 150, clipped to 142, provided by external core. Mappers =  
951 Minimap2 (better), BWA-MEM.

952 Supplemental Figure 3E: HIV single nucleotide variants (SNVs) in pHXB2\_D, long vs. short  
953 reads (SNV-focused).

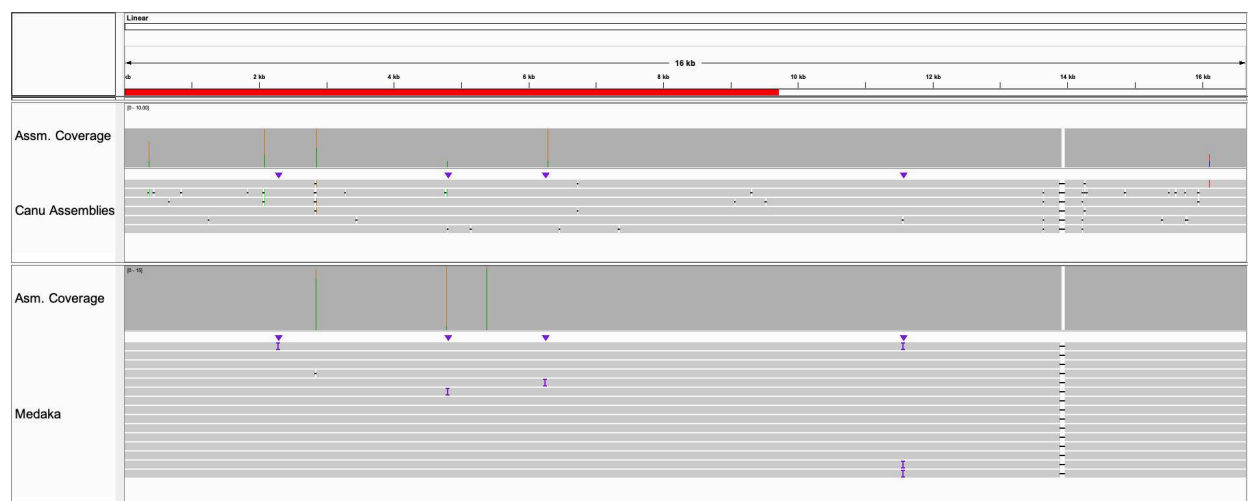
954

955 **Supplemental Figure 4A: Assembling pHXB2\_D from long reads only, varying basecaller**  
 956 **and polymerase.**

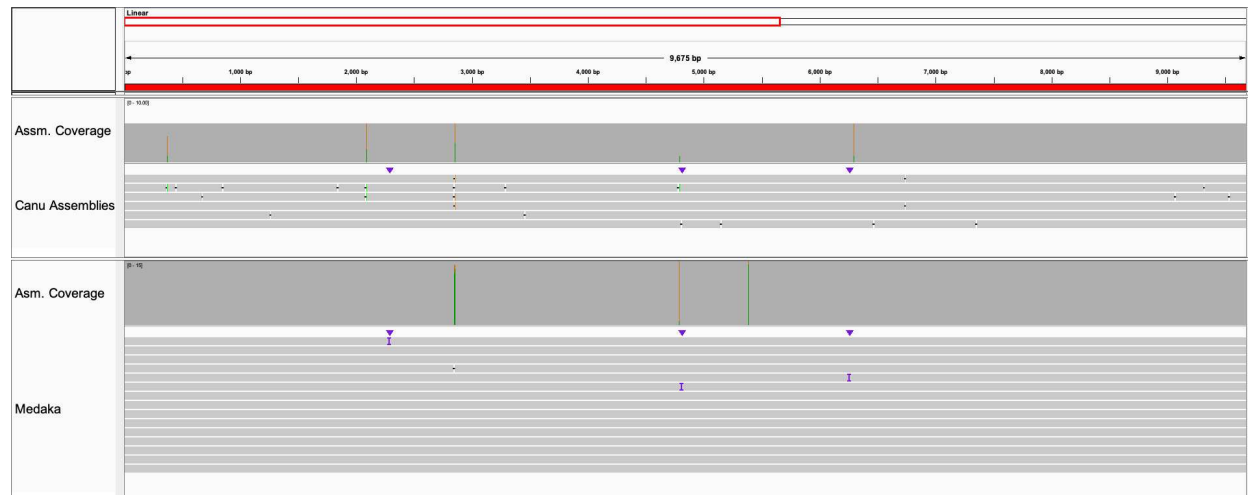


957  
 958 Each pane (n=6) summarizes the results of contig curation. Divergence from reference decreases  
 959 with newer basecallers, and with long amplicon DNA polymerase (Sigma-Aldrich Taq vs. LA  
 960 Taq by Takara). Errors in assembly occurred at homopolymers (most often deletions not visible  
 961 at this resolution; see **Supplemental Figure 6**), dimer or trimer runs. bar10 = LA Taq library.  
 962 bar11 = Taq library. pHXB2\_D Genbank:MW079479. Best contigs presented, manually curated  
 963 to match pHXB2\_D coordinates. Note LTRs (beginning and terminal 634 bp of red bar) are  
 964 resolved in almost all assemblies. See **Supplemental Table 3** for differences between assemblies  
 965 and the reference (left red). Plasmid backbone (right) differences are not reported.  
 966



967 **Supplemental Figure 4B: ONT errors corrected by polishing ONT-only assemblies.**

968



969

970 Assemblies polished with Medaka (ONT). Top: pHXB2\_D genome. Bottom: HIV-only segment.

971 The best polished assembly had one error in the entire plasmid (1 error out of 16,722 bases), with

972 a corresponding consensus accuracy of 99.99402%. This happened to be in HIV segment (HIV-1

973 between position 1 and 9719; 1 error out of 9719 bases ), with corresponding accuracy of

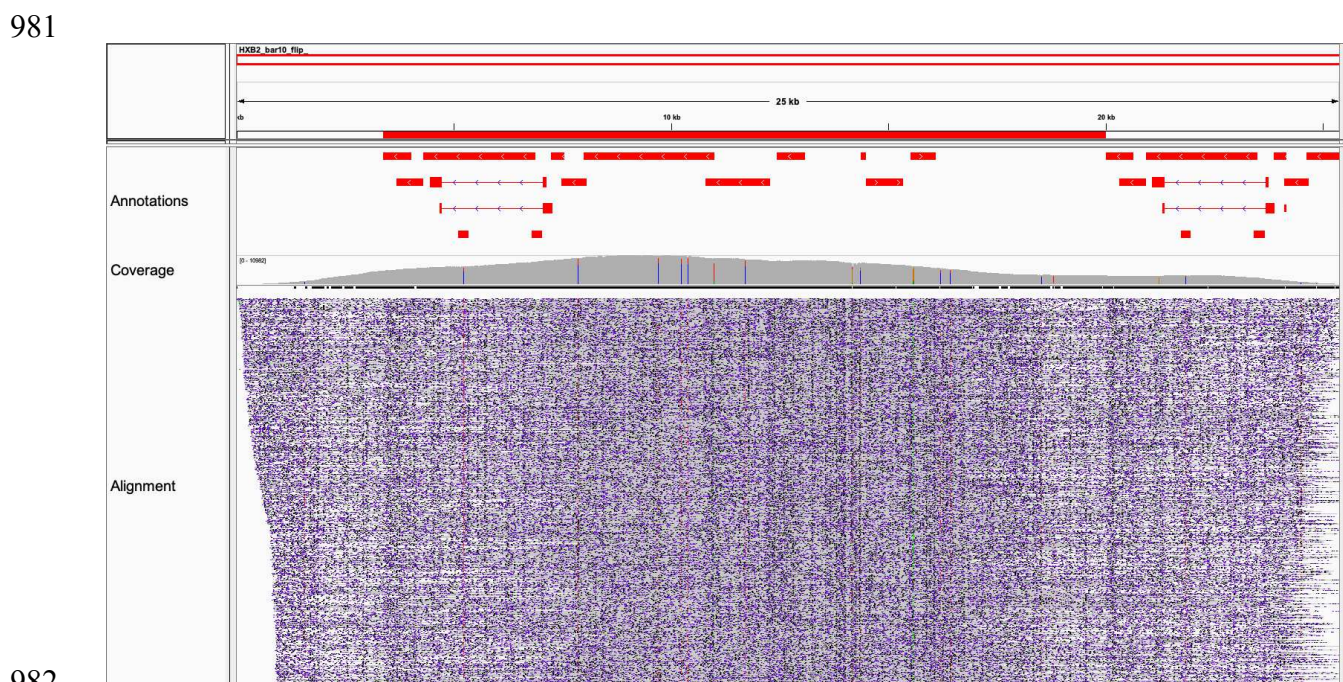
974 99.989711%. Note the conserved 52 bp gap in the backbone of pHXB2\_D was redundant

975 sequence included in the short-read assembly from the core. It was not supported by long-read

976 data, and therefor was validated as a technical artifact from the core's pipeline. Reference: short-

977 read assembly. LTRs (beginning and terminal 634 bp of red bar) are resolved in polished  
978 assemblies.

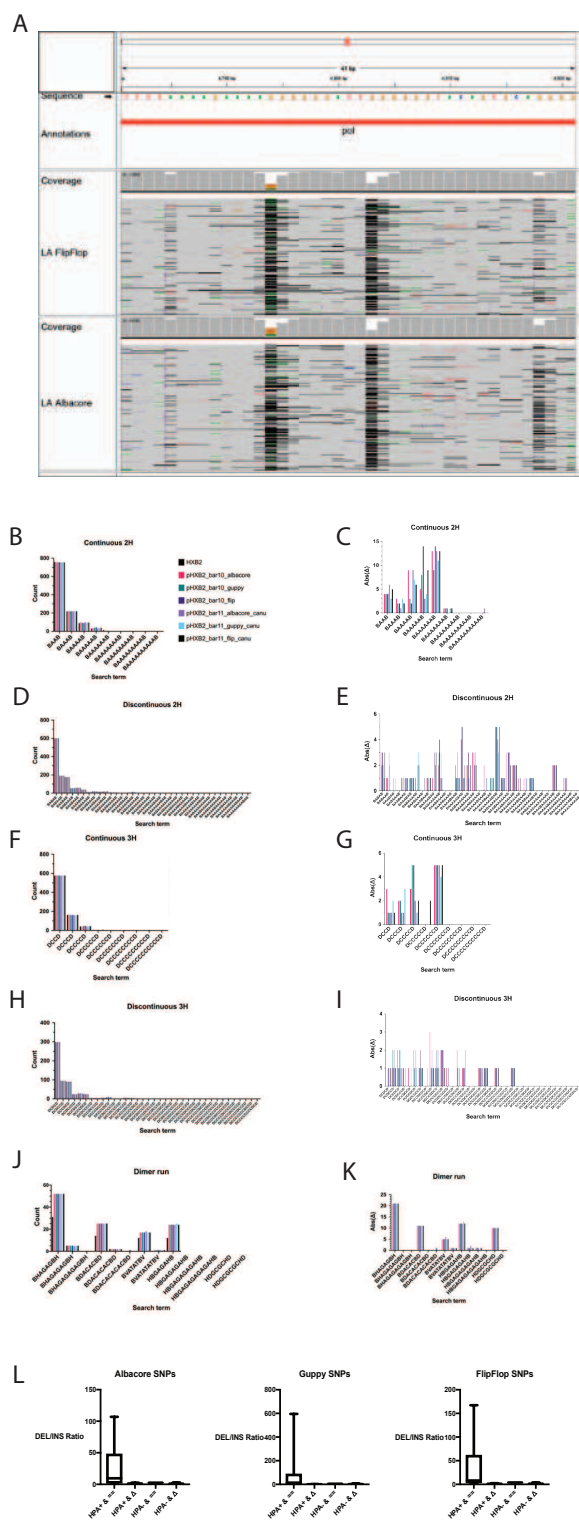
979 **Supplemental Figure 4C: Mappability of long reads over contigs during assembly quality**  
 980 **control.**



982  
 983 Coverage depends on context. Abrupt changes in coverage from terminal regions of HXB2  
 984 **(Figure 1F, Supplemental Figures 1 and 3)** were artifacts from supplying mappers with an  
 985 HIV reference without a plasmid backbone. Long reads from barcode 10 (LA Taq) mapped with  
 986 minimap2 [23] and “reference” contig from assembly (Canu v1.8) with basecalled data  
 987 (FlipFlop). Stripes in this figure are not SNVs. They represent technical variability at  
 988 homopolymers. Assemblies were manually curated to start with 5’ LTR in the sense orientation,  
 989 leaving the plasmid backbone on the left. Because there were not real insertions in the HIV  
 990 segment, the HIV coordinates are the same as HXB2 (both 9719 bp long). Compare with 52 bp  
 991 technical artifact from the core’s short read assembly in **Supplemental Figure 4A, 4B.**

992

993 Supplemental Figure 5: Homopolymers and dimer runs are ONT artifacts in unpolished  
 994 assemblies.



995

996 Supplemental Figure 5A: A set of homopolymer tracks from HXB2 plasmid. Alignments with  
997 BWA-MEM shown from FlipFlop (top) and Albacore (bottom) basecalled reads. Mapping is  
998 pre-assembly.

999 Supplemental Figure 5B: Continuous 2H counts in unpolished assemblies. 2H = A or T  
1000 homodimers.

1001 Supplemental Figure 5C: Continuous 2H Absolute Difference.

1002 Supplemental Figure 5D: Discontinuous 2H counts in unpolished assemblies.

1003 Supplemental Figure 5E: Discontinuous 2H Absolute Difference.

1004 Supplemental Figure 5F: Continuous 3H counts in unpolished assemblies. 3H = C or G  
1005 homodimers.

1006 Supplemental Figure 5G: Continuous 3H Absolute Difference.

1007 Supplemental Figure 5H: Discontinuous 3H counts in unpolished assemblies.

1008 Supplemental Figure 5I: Discontinuous 3H Absolute Difference.

1009 Supplemental Figure 5J: Dimer run counts in unpolished assemblies.

1010 Supplemental Figure 5K: Dimer run Absolute Difference. Dimer runs as pairs are the most  
1011 problematic, with runs as triplets being resolvable by ONT.

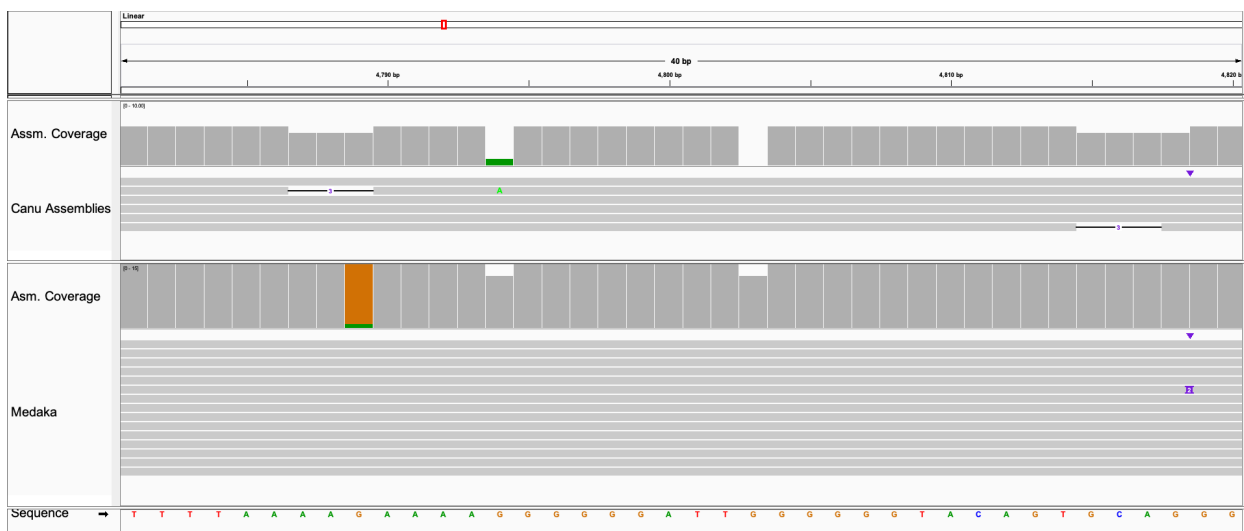
1012 Supplemental Figure 5L: The ratio of deletions to insertions is higher at mismatches both  
1013 adjacent to homopolymers and similar to neighbor bases. Box plot shows median (“x” is mean)  
1014 and quartile ranges. Y-axis is ratio. HPA: homopolymer-adjacent. ==: same as neighbor base. Δ:  
1015 different than neighbor base. Higher coverage (above ~10) usually makes up for current error  
1016 profile. Above true for Albacore, Guppy, and FlipFlop.

1017 **Supplemental Figure 6: Assembly partially resolved homopolymers, which are improved**  
 1018 **by polishing**

1019



1020



1021 Top: Six ONT-only assemblies. Bottom: polished ONT-only assemblies, varying Medaka  
 1022 models. Deletions at 5' of G homopolymers were not corrected, regardless of basecaller or Taq  
 1023 isoform. Note that polishing was not performed. IGV window is Linear:4,781-4,820. Bottom:

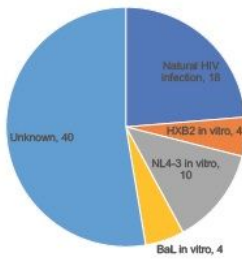
1024 polishing canu assemblies with medaka abrogated most ONT artifacts. Best medaka setting

1025 tested: r941\_min\_high\_g330.

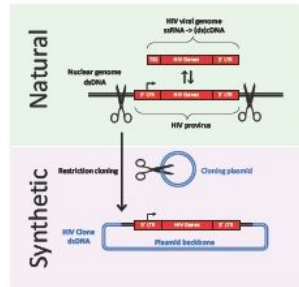
1026

# Figures

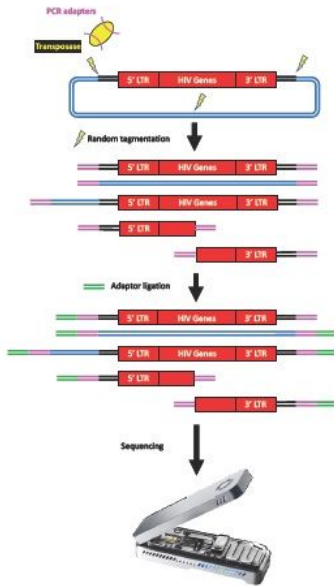
A



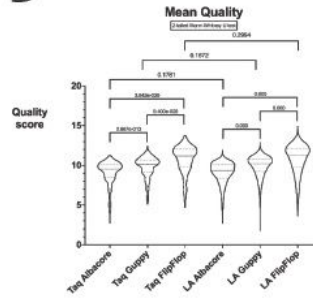
B



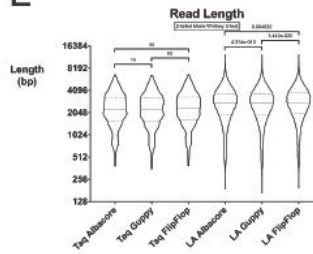
C



D



E



F

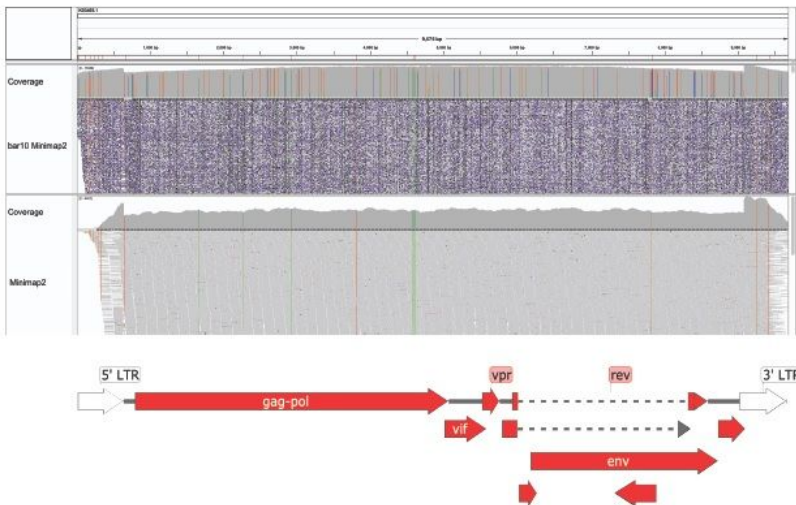


Figure 1

HIV information in pHXB2\_D is recovered by long-read sequencing and mapping. Figure 1A: HXB2 is still a commonly used resource. It is the reference HIV-1 genome, derived from one of the earliest clinical isolates. While older HIV samples are occasionally rediscovered, they are not made routinely available to



researchers. All public HIV-1 RNA-seq datasets were obtained from the NCBI SRA with the following search phrase: "HIV-1" AND "RNA-seq". Metadata from these 2527 runs (number current as of 7/21/2020) were used to make a pie chart summary. Figure 1B: HIV information comes from three main sources: proviruses (HIV sandwiched between two assumedly identical full-length long terminal repeats (LTRs)), unspliced HIV mRNAs (also known as viral genomes) starting from the transcription start site and ending in the 3' LTR [4], and engineered proviruses recovered in their entirety or stitched together from multiple isolates like NL4-3 [18]. Figure 1C: ONT library prep pipeline. Tagmentation cleaves double-stranded DNA, ligating barcoded PCR adapters (magenta). PCR-adapted DNA may be amplified. After amplification and cleanup, ONT sequencing adapters (green) are ligated. Barcoded samples may be pooled and sequenced. Figure 1D: Newer basecallers increase read mean quality. Median (big dash) and quartiles (little dash). Effect of enzyme version was not statistically significant. Figure 1E: Read stats with different callers/aligners. Median (big dash) and quartiles (little dash). Read lengths increase with higher fidelity Taq. Figure 1F: Sequencing coverage with long- vs. short-read single-end 150 bp (trimmed to 142 bp) DNA sequencing. Long-read sequencing covers ambiguously mappable areas missed by short read in HXB2 reference Genbank:K03455.1 (Supplemental Figures 3D,3E), but at the expense of accuracy near homopolymers longer than about 4 nucleobases (Supplemental Figure 5). Short-read mapping fails at repetitive elements longer than their read lengths (Supplemental Figures 3D,3E). Long read Minimap2 settings: map-ont -k15. Short read Minimap2 settings: Short reads without splicing (-k21 -w11 -sr -F800 -A2 -B8 -O12,32 -E2,1 -r50 -p.5 -N20 -f1000,5000 -n2 -m20 -s40 -g200 -2K50m -heap-sort=yes -secondary=no) (sr).





100% coverage and 93.02% identity to HIV-1 HXB2. This read was 11,487 bases long, with mean quality score 11.984396. Basecalled using Guppy 2.3.1 with FlipFlop config.

```

CLUSTAL format alignment by MAFFT (v7.475)

K03455.1_5'LTR  tggagggttaattcactcccaagaagaagacaagatattcctgatctgtggatctaccaca
pHXB2_D_5'LTR  tggagggttaattcactcccaagaagaagacaagatattcctgatctgtggatctaccaca
pHXB2_D_3'LTR  tggagggttaattcactcccaagaagaagacaagatattcctgatctgtggatctaccaca
K03455.1_3'LTR  tggagggttaattcactcccaagaagaagacaagatattcctgatctgtggatctaccaca
*****

K03455.1_5'LTR  cacaaggctacttccctgattagcagaactcacaccagggccagggtcagatattccac
pHXB2_D_5'LTR  cacaaggctacttccctgattagcagaactcacaccagggccagggtcagatattccac
pHXB2_D_3'LTR  cacaaggctacttccctgattagcagaactcacaccagggccagggtcagatattccac
K03455.1_3'LTR  cacaaggctacttccctgattagcagaactcacaccagggccagggtcagatattccac
*****

K03455.1_5'LTR  tgaccttggatggtgtcacaagctagtaccagttgagccagagaagttagaagaagcca
pHXB2_D_5'LTR  tgaccttggatggtgtcacaagctagtaccagttgagccagagaagttagaagaagcca
pHXB2_D_3'LTR  tgaccttggatggtgtcacaagctagtaccagttgagccagagaagttagaagaagcca
K03455.1_3'LTR  tgaccttggatggtgtcacaagctagtaccagttgagccagagaagttagaagaagcca
*****

K03455.1_5'LTR  acaaaggagagaaccaccagcttggttacacctgtgagcctgcatggaatggatgaccgg
pHXB2_D_5'LTR  acaaaggagagaaccaccagcttggttacacctgtgagcctgcatggaatggatgaccgg
pHXB2_D_3'LTR  acaaaggagagaaccaccagcttggttacacctgtgagcctgcatggaatggatgaccgg
K03455.1_3'LTR  acaaaggagagaaccaccagcttggttacacctgtgagcctgcatggaatggatgaccgg
*****

K03455.1_5'LTR  agagagaagtgttagagtgagggttggacagccgctagcatttcatcacatggcccag
pHXB2_D_5'LTR  agagagaagtgttagagtgagggttggacagccgctagcatttcatcacatggcccag
pHXB2_D_3'LTR  agagagaagtgttagagtgagggttggacagccgctagcatttcatcacatggcccag
K03455.1_3'LTR  agagagaagtgttagagtgagggttggacagccgctagcatttcatcacatggcccag
*****

K03455.1_5'LTR  agctgcatccggagtacttcaagaactgctgacatcgagcttggctacaaggactttccg
pHXB2_D_5'LTR  agctgcatccggagtacttcaagaactgctgacatcgagcttggctacaaggactttccg
pHXB2_D_3'LTR  agctgcatccggagtacttcaagaactgctgacatcgagcttggctacaaggactttccg
K03455.1_3'LTR  agctgcatccggagtacttcaagaactgctgacatcgagcttggctacaaggactttccg
*****

K03455.1_5'LTR  ctggggactttccaggaggcgtggcctggggcgggactggggagtgggcgagccctcagat
pHXB2_D_5'LTR  ctggggactttccaggaggcgtggcctggggcgggactggggagtgggcgagccctcagat
pHXB2_D_3'LTR  ctggggactttccaggaggcgtggcctggggcgggactggggagtgggcgagccctcagat
K03455.1_3'LTR  ctggggactttccaggaggcgtggcctggggcgggactggggagtgggcgagccctcagat
*****

K03455.1_5'LTR  cctgcataaagcagctgcttttggctgactgggtctctctggttagaccagatctga
pHXB2_D_5'LTR  cctgcataaagcagctgcttttggctgactgggtctctctggttagaccagatctga
pHXB2_D_3'LTR  cctgcataaagcagctgcttttggctgactgggtctctctggttagaccagatctga
K03455.1_3'LTR  cctgcataaagcagctgcttttggctgactgggtctctctggttagaccagatctga
*****

K03455.1_5'LTR  gctggggactctctggctaaactagggaaccactgcttaagcctcaataaagcttgct
pHXB2_D_5'LTR  gctggggactctctggctaaactagggaaccactgcttaagcctcaataaagcttgct
pHXB2_D_3'LTR  gctggggactctctggctaaactagggaaccactgcttaagcctcaataaagcttgct
K03455.1_3'LTR  gctggggactctctggctaaactagggaaccactgcttaagcctcaataaagcttgct
*****

K03455.1_5'LTR  tgagtgctcaagtagtgtgtgcccctctgtgtgtgactctggttaactagagatccctc
pHXB2_D_5'LTR  tgagtgctcaagtagtgtgtgcccctctgtgtgtgactctggttaactagagatccctc
pHXB2_D_3'LTR  tgagtgctcaagtagtgtgtgcccctctgtgtgtgactctggttaactagagatccctc
K03455.1_3'LTR  tgagtgctcaagtagtgtgtgcccctctgtgtgtgactctggttaactagagatccctc
*****

K03455.1_5'LTR  agacccttttagtcagtggtgaaaatctctagca
pHXB2_D_5'LTR  agacccttttagtcagtggtgaaaatctctagca
pHXB2_D_3'LTR  agacccttttagtcagtggtgaaaatctctagca
K03455.1_3'LTR  agacccttttagtcagtggtgaaaatctctagca
*****

```

```

CLUSTAL format alignment by MAFFT (v7.475)

AF324493.1_5LTR tggagggttaatttggcccccaagaagaagacaagatattcctgatctgtggatctaccaca
ACCESSION_TBD_5 tggagggttaatttggcccccaagaagaagacaagatattcctgatctgtggatctaccaca
AF324493.1_3LTR tggagggttaatttggcccccaagaagaagacaagatattcctgatctgtggatctaccaca
ACCESSION_TBD_3 tggagggttaatttggcccccaagaagaagacaagatattcctgatctgtggatctaccaca
*****

AF324493.1_5LTR  cacaaggctacttccctgattggcagaactcacaccagggccagggtcagatattccac
ACCESSION_TBD_5 cacaaggctacttccctgattggcagaactcacaccagggccagggtcagatattccac
AF324493.1_3LTR  cacaaggctacttccctgattggcagaactcacaccagggccagggtcagatattccac
ACCESSION_TBD_3 cacaaggctacttccctgattggcagaactcacaccagggccagggtcagatattccac
*****

AF324493.1_5LTR  tgaccttggatggtgtcacaagctagtaccagttgagccagagaagttagaagaagcca
ACCESSION_TBD_5 tgaccttggatggtgtcacaagctagtaccagttgagccagagaagttagaagaagcca
AF324493.1_3LTR  tgaccttggatggtgtcacaagctagtaccagttgagccagagaagttagaagaagcca
ACCESSION_TBD_3 tgaccttggatggtgtcacaagctagtaccagttgagccagagaagttagaagaagcca
*****

AF324493.1_5LTR  atgaaggagagaacaacacagcttggttacacctatgagccagatgggtagggagaccgg
ACCESSION_TBD_5 atgaaggagagaacaacacagcttggttacacctatgagccagatgggtagggagaccgg
AF324493.1_3LTR  atgaaggagagaacaacacagcttggttacacctatgagccagatgggtagggagaccgg
ACCESSION_TBD_3 atgaaggagagaacaacacagcttggttacacctatgagccagatgggtagggagaccgg
*****

AF324493.1_5LTR  agggagaagtattagtgtggaagtggacagcctctagcatttctcactgcccag
ACCESSION_TBD_5 agggagaagtattagtgtggaagtggacagcctctagcatttctcactgcccag
AF324493.1_3LTR  agggagaagtattagtgtggaagtggacagcctctagcatttctcactgcccag
ACCESSION_TBD_3 agggagaagtattagtgtggaagtggacagcctctagcatttctcactgcccag
*****

AF324493.1_5LTR  agctgcatccggagtacttcaagaactgctgacatcgagcttggctacaaggactttccg
ACCESSION_TBD_5 agctgcatccggagtacttcaagaactgctgacatcgagcttggctacaaggactttccg
AF324493.1_3LTR  agctgcatccggagtacttcaagaactgctgacatcgagcttggctacaaggactttccg
ACCESSION_TBD_3 agctgcatccggagtacttcaagaactgctgacatcgagcttggctacaaggactttccg
*****

AF324493.1_5LTR  ctggggactttccaggaggcgtggcctggggcgggactggggagtgggcgagccctcagat
ACCESSION_TBD_5 ctggggactttccaggaggcgtggcctggggcgggactggggagtgggcgagccctcagat
AF324493.1_3LTR  ctggggactttccaggaggcgtggcctggggcgggactggggagtgggcgagccctcagat
ACCESSION_TBD_3 ctggggactttccaggaggcgtggcctggggcgggactggggagtgggcgagccctcagat
*****

AF324493.1_5LTR  gctacataaagcagctgcttttggctgactgggtctctctggttagaccagatctga
ACCESSION_TBD_5 gctacataaagcagctgcttttggctgactgggtctctctggttagaccagatctga
AF324493.1_3LTR  gctacataaagcagctgcttttggctgactgggtctctctggttagaccagatctga
ACCESSION_TBD_3 gctacataaagcagctgcttttggctgactgggtctctctggttagaccagatctga
*****

AF324493.1_5LTR  gctggggactctctggctaaactagggaaccactgcttaagcctcaataaagcttgct
ACCESSION_TBD_5 gctggggactctctggctaaactagggaaccactgcttaagcctcaataaagcttgct
AF324493.1_3LTR  gctggggactctctggctaaactagggaaccactgcttaagcctcaataaagcttgct
ACCESSION_TBD_3 gctggggactctctggctaaactagggaaccactgcttaagcctcaataaagcttgct
*****

AF324493.1_5LTR  tgagtgctcaagtagtgtgtgcccctctgtgtgtgactctggttaactagagatccctc
ACCESSION_TBD_5 tgagtgctcaagtagtgtgtgcccctctgtgtgtgactctggttaactagagatccctc
AF324493.1_3LTR  tgagtgctcaagtagtgtgtgcccctctgtgtgtgactctggttaactagagatccctc
ACCESSION_TBD_3 tgagtgctcaagtagtgtgtgcccctctgtgtgtgactctggttaactagagatccctc
*****

AF324493.1_5LTR  agacccttttagtcagtggtgaaaatctctagca
ACCESSION_TBD_5 agacccttttagtcagtggtgaaaatctctagca
AF324493.1_3LTR  agacccttttagtcagtggtgaaaatctctagca
ACCESSION_TBD_3 agacccttttagtcagtggtgaaaatctctagca
*****

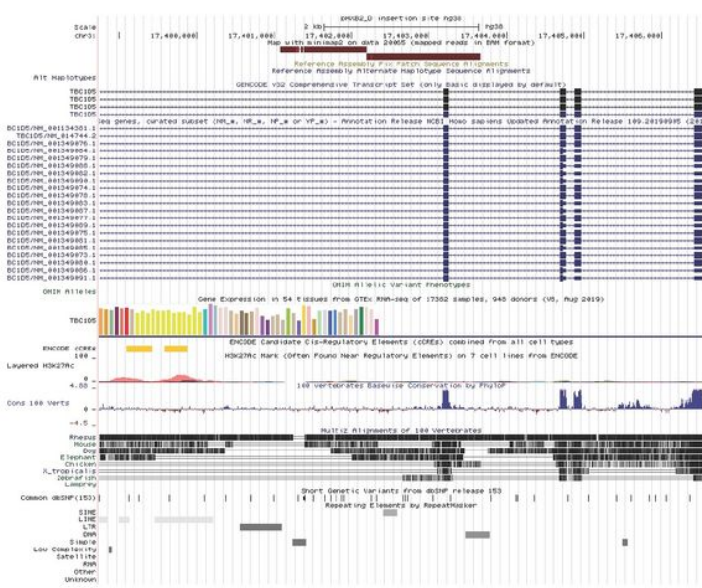
```

3A

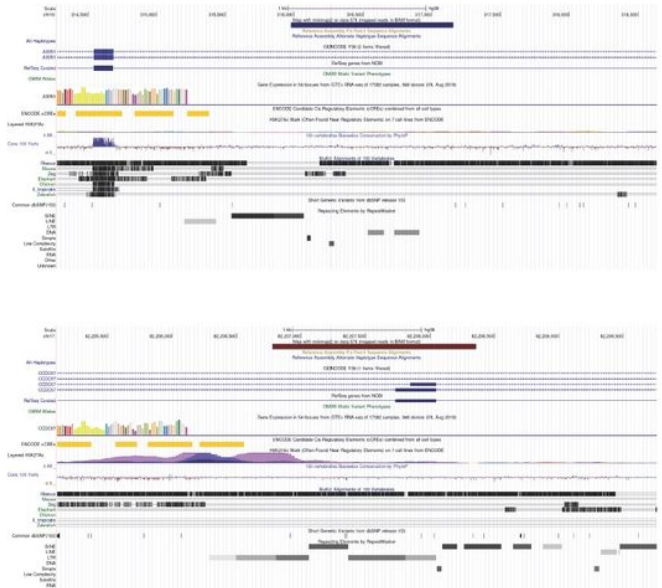
3B

Figure 3

3A: pHXB2\_D has identical LTRs, resolving likely errors in HXB2 (K03455.1) 3B: pNL4-3\_gag-pol(Δ1443-4553)\_EGFP (ACCESSION\_TBD) has distinct LTRs, consistent with pNL4-3 (AF324493.1)



4A



4B

**Figure 4**

4A: HXB2 integration site 4B: NL4-3 integration sites Figure 4A: pHXB2\_D's, and therefore HXB2's, integration site is unambiguously singular (falls outside of annotated repeat), and in the same orientation (minus strand relative to hg38) as target gene TBC1D5. Alignment quality is 60 for both homology arms (Supplemental Table 2). Features captured by homology arms in pHXB2\_D and other clones verified as proviruses in the present study are consistent with HIV-1 integration behavior [44]. Visualized in UCSC Genome Browser [45]. Figure 4B: pNL4-3\_gag-pol( $\Delta$ 1443-4553)\_EGFP's, and therefore NL4-3's, integration sites fall on annotated repeats, the longer reads help to locate both sites. Alignment quality is 60 for both homology arms (Supplemental Table 2). These integration sites would likely be missed by any method leveraging reads shorter than the homology arms.

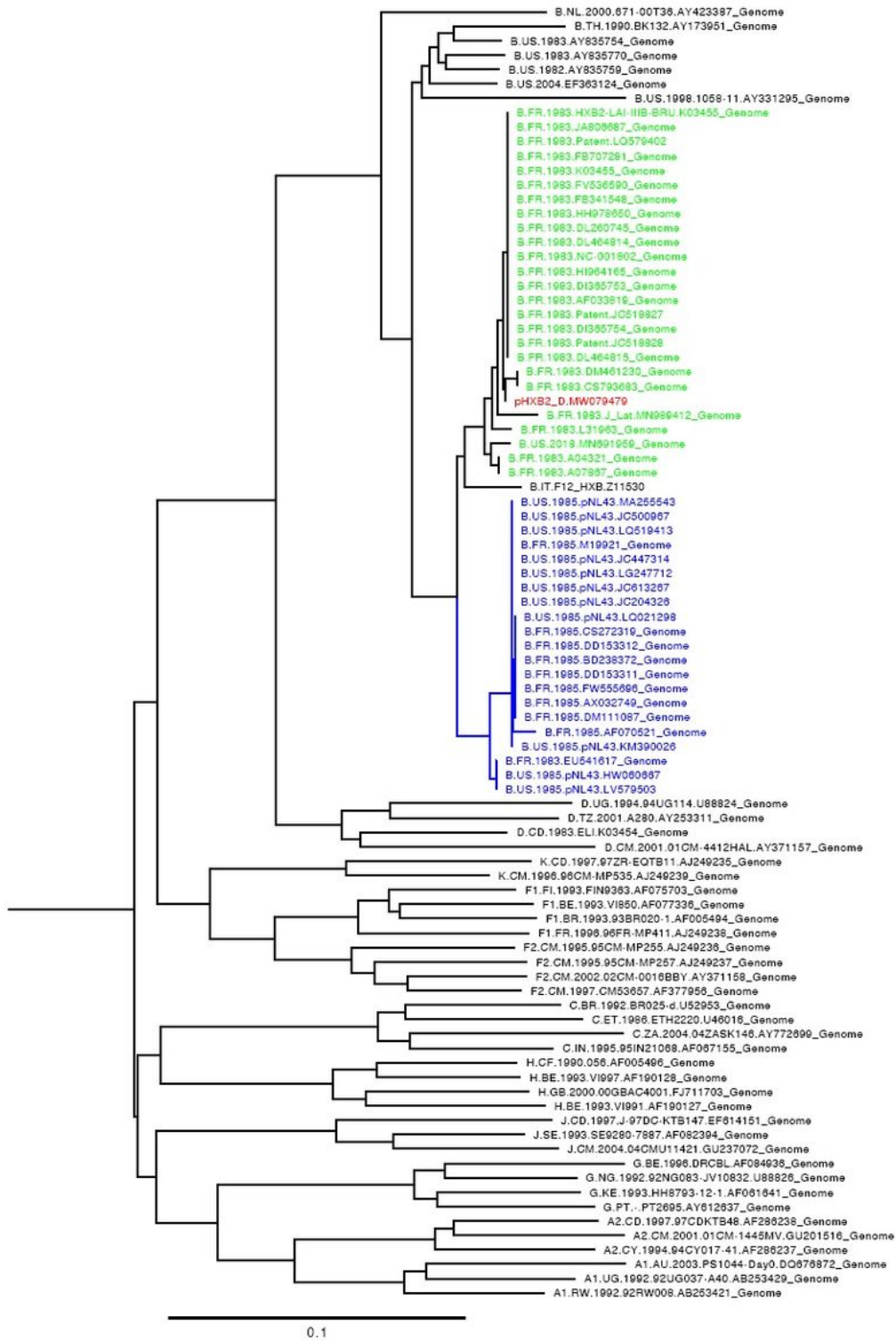
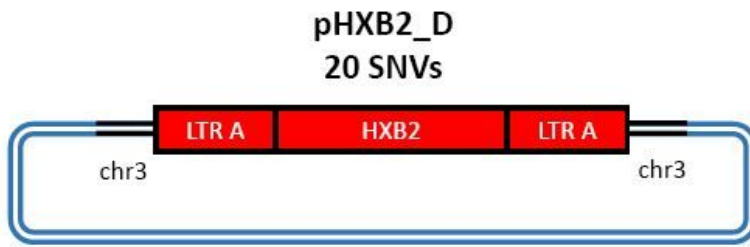


Figure 5

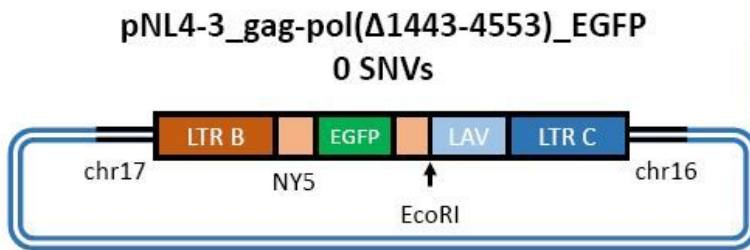
pHXB2\_D provenance and top 50 neighbors



Stabilized provirus



Transient recombinant



LTR phasing success		
	pHXB2_D	pNL4-3 $\Delta$
ONT PCR barcode	Yes	Yes
ILMN SE 150 barcode	Yes*	Yes

LTR C takes over in subsequent viruses.

\*intermittent success with ambiguous mapping at LTR.

Figure 6

Summary of long- vs. short-read mapping by ability to phase LTRs

## Supplementary Files

This is a list of supplementary files associated with this preprint. Click to download.

- [SupplementalInformation.pdf](#)
- [Generetal.pHXB2DTablesandSupplementalTables.xlsx](#)